



JAAS

**Chromatography Purification of Rb for Accurate Isotopic Analysis by MC-ICPMS: A Comparison between AMP-PAN, Cation-Exchange, and Sr Resins**

Journal:	<i>Journal of Analytical Atomic Spectrometry</i>
Manuscript ID	JA-ART-07-2021-000268.R1
Article Type:	Paper
Date Submitted by the Author:	20-Sep-2021
Complete List of Authors:	Nie, Nicole; Carnegie Institution for Science; The University of Chicago Dauphas, Nicolas; The University of Chicago Hopp, Timo; The University of Chicago Hu, Justin; The University of Chicago Zhang, Zhe; The University of Chicago Yokochi, Reika; The University of Chicago Ireland, Thomas; Boston University; The University of Chicago Tissot, François L.H.; California Institute of Technology; The University of Chicago

SCHOLARONE™  
Manuscripts

# Chromatography Purification of Rb for Accurate Isotopic Analysis by MC-ICPMS: A Comparison between AMP-PAN, cation-exchange, and Sr resins

Nicole X. Nie<sup>1,2\*</sup>, Nicolas Dauphas<sup>1</sup>, Timo Hopp<sup>1</sup>, Justin Y. Hu<sup>1</sup>, Zhe J. Zhang<sup>1</sup>, Reika Yokochi<sup>1</sup>, Tom Ireland<sup>1,3</sup>, Francois L. H. Tissot<sup>1,4</sup>

<sup>1</sup>Department of the Geophysical Sciences and Enrico Fermi Institute, The University of Chicago, Chicago, IL 60637

<sup>2</sup>Earth and Planets Laboratory, Carnegie Institution for Science, Washington, DC 20015

<sup>3</sup>Department of Earth and Environment, Boston University, Boston, MA 02215

<sup>4</sup>The Isotoparium, Division of Geological and Planetary Sciences, California Institute of Technology, Pasadena, CA 91125

\*To whom correspondence should be addressed ([nnie@carnegiescience.edu](mailto:nnie@carnegiescience.edu))

## Abstract

The isotopic compositions of alkali metal elements are powerful tracers of various geological processes. Coupled K and Rb isotopic studies can potentially yield new clues on the mechanisms responsible for the depletions in moderately volatile elements in planetary objects, global surface geochemical cycles, and mechanistic aspects of water-rock interactions. Rubidium isotopic studies have however been hampered by difficulties in purifying Rb from rocks, notably due to its similar chemical behavior to K. Here we characterize the properties of three different types of resins (AMP-PAN resin; AG50W-X8 and AG50W-X12 cation-exchange resins; Sr resin) for Rb and K purification. We show that AMP-PAN resin and Sr resin can readily separate Rb from K and other matrix elements. However, AMP-PAN resin has a high Rb blank (~80 ng) and is cumbersome to use, which limits its applicability. For cation resins, we test the effects of column length, acid molarity, temperature, pressure drop (flow rate), and resin cross-linkage on the Rb separation using a Fluoropolymer Pneumatic Liquid Chromatography (FPLC) unit built in our laboratory. Increasing column length or resin cross-linkage has a positive effect on the separation, while increasing acid molarity, temperature, or pressure drop (flow rate) has negative impacts. Gravity-driven cation-exchange resin columns fail to cleanly separate Rb from K, but an AG50W-X12 resin column of 150 cm length and 0.16 cm inner diameter installed on a FPLC unit can cleanly separate Rb from K. We separated Rb from synthetic and natural rocks samples using three different purification schemes designed based on the three types of resins, and measured the Rb isotopic compositions of the Rb separates by MC-ICPMS. The three methods yielded consistent results, demonstrating the efficacy of our Rb separation and the accuracy of our Rb isotopic analyses. The Rb isotopic compositions of several

1  
2  
3  
4 35 geostandards were analyzed (BCR-2, BHVO-2, BE-N, AGV-2, GS-N, G-3, and G-A), which can be used in  
5 36 future studies for ground truthing methodologies used for studying natural samples. Among the three  
6 37 methods, the Sr resin method is the most straightforward for purifying Rb and K simultaneously, and  
7 38 measuring their isotopic compositions in natural samples.  
9 39

## 1. Introduction

Alkali metals (Li, Na, K, Rb, Cs, and unstable Fr) are a group of elements that have found considerable use in geochemistry and cosmochemistry. They are univalent, redox insensitive, moderately volatile, lithophile, and fluid mobile. Among them, Li, K, and Rb have at least two stable or long-lived isotopes, and measurements of their isotopic ratios by multi-collector inductively coupled plasma mass spectrometry (MC-ICPMS) have provided new insights into geochemical processes such as volatile element depletion during planetary formation, continental crust extraction and recycling by subduction, and surface weathering and climate feedbacks (*e.g.*, ref. 1–21, and references therein).

A major obstacle to the routine isotopic analysis of these alkali elements by MC-ICPMS is the presence of potential isobaric interferences and matrix effects that can cause changes in instrumental mass-bias. It is therefore critical to purify the element of interest using ion exchange chromatography prior to isotopic analysis. Purifying Li and K is relatively straightforward (*e.g.*, ref. 2,9,11,22–24). However, purifying Rb from rocks for high-precision isotopic analyses is rather difficult, mostly because it is a trace element that follows K closely in aqueous chemistry. This is not a problem for K isotopic analysis because the weight K/Rb ratio in terrestrial rocks and meteorites ranges from ~50 to 1000<sup>25</sup>, so Rb does not need to be separated for K isotopic analysis<sup>26</sup>. The opposite is not true, as precise Rb isotopic analysis by MC-ICPMS requires a K/Rb ratio of less than 10<sup>14</sup>. An additional challenge is that Rb has only two stable isotopes, <sup>85</sup>Rb and <sup>87</sup>Rb (with isotopic abundances of 72.17 and 27.83%, respectively), meaning that a double spike technique<sup>27</sup> cannot be used to correct for potential isotopic fractionation during chromatographic purification and MC-ICPMS analysis. A high Rb yield is therefore essential for minimizing isotopic fractionation during chromatography<sup>28</sup> and obtaining accurate Rb isotopic data.

Studies on Rb stable isotopes (*i.e.*, <sup>87</sup>Rb/<sup>85</sup>Rb ratios) are so far very limited, despite its great potential for probing diverse geological and planetary processes. Waight et al.<sup>29</sup> used a Zr-doping method for the determination of Rb isotopic compositions by MC-ICPMS. Nebel et al.<sup>30</sup> applied this method to Rb-enriched natural samples such as mica and granites, and obtained a precision of ~±0.5‰ on the <sup>87</sup>Rb/<sup>85</sup>Rb ratio. Nebel et al.<sup>6</sup> measured chondrites using the same method and found no Rb isotopic variation among the samples within ±1‰. Pringle and Moynier<sup>12</sup> used cation exchange chromatography to separate Rb from rock matrices but they reported no elution curve, and it is unclear whether Rb was efficiently separated from K in that study. They reported a precision of Rb MC-ICPMS analysis of ~±0.05‰, and found small isotopic differences between terrestrial rocks, lunar samples, and chondrites, some of which have been replicated by Nie and Dauphas<sup>14</sup>. Zhang et al.<sup>28</sup> developed a Rb chromatography purification method using a single Sr resin column and applied it to several geostandards. Building on that work, Nie and Dauphas<sup>14</sup> achieved a cleaner separation of Rb from K and other matrix elements for study of Rb-depleted samples by using more elongated columns, and reported Rb isotopic analyses of lunar samples with precisions of ~±0.05‰. Combining these data with K isotope data reported previously<sup>10</sup>, Nie and Dauphas<sup>14</sup> concluded that vapor drainage from the protolunar disk onto the Earth was the most likely cause for lunar volatile element depletion. Rubidium isotopic analysis may also find some applications in studies of surface

1  
2  
3  
4 77 weathering<sup>31</sup>. Almost all analyses of terrestrial samples so far have focused on geostandards and igneous  
5 78 rocks which have relatively abundant Rb<sup>12,14,28,30</sup>, and a reliable chemical purification method is required  
6 79 for the broader applications of Rb isotopes.

8 80 Three resins have been used in the literature for purifying Rb, including AMP-PAN resin<sup>32,33</sup>, cation-  
9 81 exchange resins<sup>6,12</sup>, and Sr resin<sup>14,28</sup>. In this work, we test the effectiveness of these three resins. We also  
10 82 develop three complete Rb separation procedures using the three resins, and apply them to synthetic and  
11 83 natural samples, which allow us to test the accuracy of the obtained Rb isotopic compositions through  
12 84 cross-comparison.

13  
14  
15 85

16  
17 86

## 18 87 **2. Materials and methods**

### 19 20 88 **2.1 Reagents and columns**

21 89 Nitric (HNO<sub>3</sub>) and hydrochloric (HCl) acids of analytical grade were double-distilled in a two-stage  
22 90 quartz-fluoropolymer sub-boiling distillation unit before use. High purity (99.999%) ammonium salts  
23 91 (ammonium nitrate and ammonium chloride) were used for making NH<sub>4</sub>NO<sub>3</sub> and NH<sub>4</sub>Cl solutions. Teflon  
24 92 labware was cleaned with water and aqua regia (concentrated acid mixture of 3:1 HCl and HNO<sub>3</sub> in volume)  
25 93 before use. Milli-Q water (18.2 MΩ.cm at 25 °C) was used for diluting acids, dissolving ammonium salts,  
26 94 and cleaning. We used different empty columns for packing the ion exchange resins and testing the  
27 95 separation of Rb. These included disposable Bio-Rad 10 mL Poly-Prep columns and 20 mL Econo-Pac  
28 96 columns, Perfluoroalkoxy alkane (PFA) columns from Savillex with inner diameter (ID) of 0.45 cm and  
29 97 customized lengths of 10–40 cm, and home-made PFA columns with 0.16 cm ID and various lengths of  
30 98 70–150 cm (for using in the fluoropolymer pneumatic liquid chromatography (FPLC) system; see Sect. 2.3).

31  
32  
33  
34  
35 99

### 36 37 38 100 **2.2 AMP-PAN resin**

39 101 The AMP-PAN resin was purchased from Eichrom. The effective component of the AMP-PAN resin  
40 102 is Ammonium MolybdoPhosphate (AMP), which is an inorganic ion exchanger with a microcrystalline  
41 103 structure. In the AMP-PAN resin, those microcrystallites are embedded in an organic matrix of  
42 104 polyacrylnitrile (PAN) to better control fluid flow and resin-fluid exchange<sup>32,33</sup>. Ammonium heteropolyacid  
43 105 salts have long been known for their cation exchange properties for alkali metal ions<sup>34</sup>. Among them, AMP  
44 106 shows great potential in separating alkali metals<sup>32,33</sup>. The principle behind its use is the substitution of the  
45 107 large ammonium ion NH<sub>4</sub><sup>+</sup> in the AMP by large alkali metal cations. The larger the alkali ions, the easier the  
46 108 substitution. The AMP-PAN resin therefore has very high selectivity of Cs, and is primarily used for treating  
47 109 Cs-contaminated radioactive wastes<sup>35</sup>.

48  
49  
50  
51  
52 110 Because of the microcrystalline structure of AMP, early studies mixed fine crystals of AMP with  
53 111 asbestos to achieve favorable flow rates for column chromatography<sup>32</sup>. The AMP-PAN resin from Eichrom  
54 112 embeds AMP in PAN to control the particle size and porosity. Despite its potential in separating alkali metals,

1  
2  
3  
4 113 the AMP-PAN resin has not been systematically tested for this purpose. Here we test if the resin can be  
5 114 used to separate Rb from K for isotopic analysis.

6 115 In order to optimize chromatography separation schemes, it is useful to simulate expected elution  
7  
8 116 curves on the basis of the theory of plate, which requires knowledge of partition coefficients of elements  
9 117 between the resin and eluent (*e.g.*, ref. 36,37). Because these are unknown for the AMP-PAN resin, we  
10 118 have determined the distribution coefficients for multiple selected elements (see Sect. 3.1).

11  
12 119

### 14 120 **2.3 Cation-exchange resins and the FPLC system**

15 121 The cation-exchange resins (AG50W-X8 200–400 mesh and AG50W-X12 200–400 mesh; both in  
16 122 H<sup>+</sup> form) are available from Bio-Rad. Cation-exchange resins are among the most commonly used resins  
17 123 for elemental purification in analytical chemistry, and distribution coefficients between cation-exchange  
18 124 resins and acids are well known. A complete set of distribution coefficients of elements in HCl, HNO<sub>3</sub> and  
19 125 H<sub>2</sub>SO<sub>4</sub> media on the cation resin AG50W-X8 have been previously determined<sup>38,39</sup>. Some of previous Rb  
20 126 isotope studies used cation resins<sup>6,12,30</sup> and diluted HCl to separate Rb from matrix elements, but no elution  
21 127 curves were reported. Nie and Dauphas<sup>14</sup> did a preliminary test on the Rb separation with AG50W-X8 200–  
22 128 400 mesh resin using a short column (1 mL column of 0.6 cm ID and 3.5 cm length), and showed significant  
23 129 overlap between Rb and K peaks during elution, calling for further refinements.

24 130 Several factors can contribute to the efficiency of a chromatography column, including the resin  
25 131 properties (*i.e.*, resin mesh size, cross-linkage, nature of the cation), the dimension of the column (*i.e.*,  
26 132 column length and inner diameter), the nature (*i.e.*, acid type and molarity) and velocity (flow rate) of the  
27 133 liquid eluent, and temperature. For a given volume of resin, it is preferable to use longer (thinner) columns  
28 134 as higher resolution is achievable. Columns that are relatively long and thin are difficult to run by gravity,  
29 135 but this issue can be mitigated by applying a pressure differential between the column top and bottom. In  
30 136 this work, we explore how the pressure drop (*i.e.*, the pressure difference between the column head and  
31 137 the outlet, which is directly related to flow rate), the length of the column, acid molarity, cation resin cross-  
32 138 linkage, and temperature affect Rb purification, with the goal of finding a method that efficiently separates  
33 139 Rb from K using only cation resins. Those tests include elution columns that are extremely long (70 to 150  
34 140 cm in length) and thin (0.16 cm ID), run under different pressure drops and at different temperatures. In  
35 141 order to perform these tests, we used a FPLC system that was designed, developed, and built in the Origins  
36 142 Lab at the University of Chicago<sup>36,40,41</sup>. A sketch of the FPLC system is shown in Fig. 1.

37 143 The FPLC system used in the present study is an updated version of the system described in ref.  
38 144 36 that has been used most recently for separating rare earth elements<sup>41</sup>, which are difficult to be separated  
39 145 from each other due to their similar chemical behaviors. There are several distinctive features about the  
40 146 FPLC unit that allow unprecedented separation of elements with similar behaviors: (*i*) column elution is  
41 147 automated and computer-controlled using a LabView software interface, allowing the use of very long/thin  
42 148 columns that may take long elution time, (*ii*) the liquid flow path is made of fluoropolymer that has a high  
43 149 acid resistance and a low alkali element blank, (*iii*) the elution temperature is controlled by a water

1  
2  
3  
4 150 circulation system, and can be adjusted from room temperature to 80 °C, and (*iv*) it uses high-purity N<sub>2</sub> gas  
5 151 to force the eluents through the column, and the extra pressure imposed on the column head can be  
6 152 adjusted from 0 to 70 psi (~4.8 bar) to achieve a desired flow rate.  
7

## 8 153 9 154 **2.4 Sr resin**

10 155 The Sr resin is commercially available from Eichrom. The Sr resin is composed of 4,4'(5')-di-  
11 156 butylcyclohexano 18-crown-6 (crown ether) in 1-octanol. The distribution coefficients of elements including  
12 157 alkalis in HNO<sub>3</sub> medium have been characterized by Horwitz et al.<sup>42</sup>. The distribution coefficients of alkali  
13 158 elements on the Sr resin are generally moderate or low (less than 10), with K partitioning more strongly in  
14 159 the resin than Rb. According to the distribution coefficients, the largest separation between K and Rb (*i.e.*,  
15 160 the largest relative difference between their distribution coefficients) occurs at ~2–3 M HNO<sub>3</sub>. Following  
16 161 previous work on Rb separation<sup>14,28</sup>, we use 3 M HNO<sub>3</sub> as the sample loading medium and the eluent. We  
17 162 tested three lengths of Sr columns (13, 20, and 40 cm) with an ID of 0.45 cm. A vacuum box from Eichrom  
18 163 was used to increase the flow rate.  
19  
20  
21  
22  
23

## 24 164 25 165 **2.5 Mass spectrometry**

26 166 Element concentrations were determined using the MC-ICPMS in the Origins Lab at the University  
27 167 of Chicago. Multi-element solutions were prepared with elements in equal concentrations of 100 µg/g by  
28 168 mixing single-element standard solutions. The multi-element solutions were diluted as needed for loading  
29 169 onto the columns and for using as elemental standards during concentration measurements. Elution  
30 170 aliquots were introduced into the MC-ICPMS via a dual cyclonic-Scott-type quartz spray chamber at a flow  
31 171 rate of ~100 µL/min. Peak jumping was used for measuring the concentrations of the multiple elements in  
32 172 each solution aliquot, and each element was measured for 5 cycles of 4.194 s integration time, with an idle  
33 173 time of 3 s between two different elements. Every batch of three samples was bracketed by two standards,  
34 174 and the concentrations were calculated by comparing the intensities of samples with the time-interpolated  
35 175 intensity averages of the two bracketing standards.  
36  
37  
38  
39  
40

41 176 Measurements of Rb isotopic compositions of purified Rb solutions by MC-ICPMS followed the  
42 177 general method used in ref. 14. Nie and Dauphas<sup>14</sup> used 15–25 ng/g Rb solution for measurements as  
43 178 limited amount of Rb was available in lunar samples, while we used here concentrations of ~100 ng/g as  
44 179 we are not limited by the Rb amount in the selected terrestrial samples. It is always preferred to use a more  
45 180 concentrated solution to increase the signal/noise ratio. Rubidium was measured in wet plasma mode and  
46 181 was introduced into the MC-ICPMS using a dual cyclonic-Scott-type quartz spray chamber at a flow rate of  
47 182 ~100 µL/min, yielding an <sup>85</sup>Rb signal of ~5 V or higher on a 100 ng/g solution. The major interference on  
48 183 Rb isotopes is isobaric <sup>87</sup>Sr<sup>+</sup> on <sup>87</sup>Rb<sup>+</sup>, which cannot be resolved using even the high-resolution slit. A low-  
49 184 resolution slit was therefore used for Rb isotopic analysis, but attention was paid to monitoring the amount  
50 185 of Sr present in the purified Rb solution by measuring the intensity of <sup>88</sup>Sr. For all the measurements  
51 186 reported here, an <sup>88</sup>Sr<sup>+</sup>/<sup>85</sup>Rb<sup>+</sup> intensity ratio below 5 × 10<sup>-4</sup> was achieved after Rb purification, and using  
52  
53  
54  
55  
56  
57  
58  
59  
60

1  
2  
3  
4 187 the measured  $^{88}\text{Sr}$  and assuming an  $^{87}\text{Sr}/^{88}\text{Sr}$  of 0.085 were sufficient to accurately correct for  $^{87}\text{Sr}$   
5 188 interference. Each data was collected as a single block of 25 cycles of 4.194 s integration time. Standard-  
6 189 sample bracketing was used to correct for instrumental mass-bias. Each sample (bracketed by standard)  
7  
8 190 was measured 7–10 times, the mean  $\delta^{87}\text{Rb}$  value was taken, and the uncertainty was calculated as 95%  
9 191 confidence interval (c.i.) using the formula  $2\sigma/\sqrt{n}$ , where  $n$  is the number of replicates of a sample and  $\sigma$   
10 192 the standard deviation of the  $\delta^{87}\text{Rb}$  of the standard bracketed by itself in an entire session (~10 hours). The  
11 193  $\sigma$  was quantified using the standard instead of the sample because the standard was measured many more  
12 194 times (several different samples were measured in one session and they were all bracketed by the same  
13 195 standard), so the standard deviation is better quantified. All Rb isotopic compositions are reported as  $\delta^{87}\text{Rb}$   
14 196 values, which are the per mil deviation of the  $^{87}\text{Rb}/^{85}\text{Rb}$  ratios of the samples from that of the Rb reference  
15 197 standard NIST SRM984.  
16  
17  
18  
19  
20

### 21 199 3. Results

#### 22 200 3.1 Rubidium purification using AMP-PAN resin

23  
24 201 The distribution coefficients of a group of selected elements on the AMP-PAN resin were  
25 202 determined. The distribution coefficient ( $K_d$ ) describes the partitioning of an element between the solid resin  
26 203 and the liquid eluent at equilibrium,  
27  
28  
29

$$30 205 \text{ distribution coefficient } (K_d) = \frac{C_i^{\text{resin}} \text{ per gram resin}}{C_i^{\text{solution}} \text{ per mL solution}}, \quad (1)$$

31 206  
32  
33 207 where  $C_i^{\text{resin}}$  is the concentration of an element  $i$  partitioned into the resin (in  $\text{mg g}^{-1}$  dry resin), and  $C_i^{\text{solution}}$  is  
34 208 the concentration of the element in the liquid phase (in  $\text{mg mL}^{-1}$  solution). It is not straightforward to  
35 209 determine the elemental concentration in the resin, therefore, a modified form of Eq. (1) was used to  
36 210 calculate the distribution coefficient of an element that relies solely on solution concentration  
37 211 measurements,  
38  
39  
40

$$41 212 \text{ distribution coefficient } (K_d) = \frac{V (C_{i,0}^{\text{solution}} - C_i^{\text{solution}})}{W C_i^{\text{solution}}}, \quad (2)$$

42 213  
43 214  
44 215 where  $C_{i,0}^{\text{solution}}$  and  $C_i^{\text{solution}}$  are the elemental concentrations in the liquid solution in  $\text{mg mL}^{-1}$  before and  
45 216 after equilibration, respectively.  $V$  is the volume of the solution (in mL), and  $W$  is the weight of dry resin (in  
46 217 g).  
47  
48  
49

50 218 Ammonium solutions have to be used to recover alkali elements from AMP-PAN resin, which  
51 219 involved the substitution of high-affinity  $\text{NH}_4^+$  for  $\text{K}^+$  and  $\text{Rb}^+$ . Therefore, we determined the distribution  
52 220 coefficients of elements in both  $\text{HNO}_3$  and  $\text{NH}_4\text{NO}_3$  solutions. A potential advantage of using  $\text{HNO}_3$  and  
53 221  $\text{NH}_4\text{NO}_3$  to determine the distribution coefficients, compared to  $\text{HCl}$  and  $\text{NH}_4\text{Cl}$ , is that  $\text{NH}_4\text{NO}_3$  has a higher  
54 222 solubility in water compared to  $\text{NH}_4\text{Cl}$  ( $1.5 \text{ g mL}^{-1} \text{ H}_2\text{O}$  for  $\text{NH}_4\text{NO}_3$  vs.  $\sim 0.4 \text{ g mL}^{-1} \text{ H}_2\text{O}$  for  $\text{NH}_4\text{Cl}$  at room  
55  
56  
57  
58  
59  
60

223 temperature), thus allowing for a more concentrated ammonium solution. Nevertheless, we also ran some  
224 tests with HCl and NH<sub>4</sub>Cl, bearing in mind that anions NO<sub>3</sub><sup>-</sup> and Cl<sup>-</sup> should not influence much the  
225 distribution coefficients as NH<sub>4</sub><sup>+</sup> is the main driver.

226 In preparation for batch equilibration experiments, a multi-element solution containing alkali metals  
227 Na, K, Rb, and Cs together with several other major and trace elements (Ti, Al, Mg, Ca, Sr, U, Fe, Zn) was  
228 prepared, by mixing single-element standard solutions in equal concentrations. Aliquots of the multi-  
229 element solution were transferred to PFA beakers, dried on a hotplate and re-dissolved in HNO<sub>3</sub> or NH<sub>4</sub>NO<sub>3</sub>  
230 solutions in different molarities. The molarities of the final solutions used for the batch equilibration  
231 experiments were 0.1, 1, 2, 4, 6, 8 and 10 mol L<sup>-1</sup> for HNO<sub>3</sub>, and 0.01, 0.1, 1, 2, 4, 6, 8 and 10 mol L<sup>-1</sup> for  
232 NH<sub>4</sub>NO<sub>3</sub> solutions. Each solution was added to a centrifuge tube containing ~200 mg of the dry resin for  
233 equilibration and was shaken manually every 2 hours. After ~8 hour of equilibration, the mixtures were  
234 filtered using empty Bio-Rad Poly-Prep columns to separate the liquid from the resin. The solutions were  
235 collected in PFA beakers and diluted using 0.3 M HNO<sub>3</sub> for concentration analysis by MC-ICPMS.

236 The distribution coefficients ( $K_d$ ) of elements on AMP-PAN resin as a function of HNO<sub>3</sub> and NH<sub>4</sub>NO<sub>3</sub>  
237 molarity are shown in Fig. 2, in base-10 logarithmic scale. The higher the distribution coefficient, the more  
238 strongly the element is bound to the resin and the larger eluent volume is needed to elute the element. The  
239 most salient results of our determination of the distribution coefficients are, (i) non-alkali elements have  
240 relatively low distribution coefficients in both HNO<sub>3</sub> and NH<sub>4</sub>NO<sub>3</sub> solutions, in general less than 10,  
241 suggesting that they can be released from the resin; (ii) alkali metals Na, K, Rb, and Cs have increasingly  
242 higher distribution coefficients as a function of ion size in both HNO<sub>3</sub> and NH<sub>4</sub>NO<sub>3</sub> solutions; Rb and Cs in  
243 particular have much higher distribution coefficients than other elements, suggesting that they can be  
244 strongly fixed onto the resin; (iii) differences between distribution coefficients of alkali metals at a similar  
245 HNO<sub>3</sub>/NH<sub>4</sub>NO<sub>3</sub> molarity are large, implying that they can be efficiently separated from each other, and (iv)  
246 the distribution coefficient of Rb is very high in HNO<sub>3</sub> (100–1000) but is decreased in NH<sub>4</sub>NO<sub>3</sub> solutions  
247 (Fig. 2), meaning that HNO<sub>3</sub> and NH<sub>4</sub>NO<sub>3</sub> can potentially be used as the loading medium for fixing Rb onto  
248 the resin and the eluent for recovering Rb, respectively.

249 Given the high distribution coefficient of Rb in HNO<sub>3</sub> and low distribution coefficient of Rb in NH<sub>4</sub>NO<sub>3</sub>  
250 (Fig. 2), the expectation is that a small column would be sufficient to separate Rb from other elements.  
251 Therefore, the resin columns used for testing the AMP-PAN resin have a 1 mL resin bed (0.8 cm ID and 2  
252 cm length) in Bio-Rad Poly-Prep empty columns. The tests were done first by loading 500 µL of a multi-  
253 element solution (20 µg/g of each element) onto the column in 4 M HNO<sub>3</sub>, followed by 15 mL 4 M HNO<sub>3</sub> to  
254 elute matrix elements and K, and then 20 mL 4 M NH<sub>4</sub>NO<sub>3</sub> to recover Rb (Fig. 3A). Solutions passed through  
255 the column were collected in 1 mL steps. The elution curves are shown in Fig. 3A. For easier comparison,  
256 y-axis of all elution curves in this study is normalized intensity, and the total area below an elution curve  
257 would be 1 for 100% recovery of the element. The elution curves reveal that: (i) matrix elements (*e.g.*, Na,  
258 Mg, Al, Ca, Fe, Ti) are not bound to the resin and are effectively eluted with 4M HNO<sub>3</sub>, as expected from

1  
2  
3  
4 259 their low distribution coefficients (Fig. 2), while Rb is strongly fixed to the resin, and *(ii)* Rb can be eluted in  
5 260 4 M  $\text{NH}_4\text{NO}_3$ .

6 261 Several problems were, however, noticed during the elution. The first problem is that during the  
7 262 elution of Rb with 4 M  $\text{NH}_4\text{NO}_3$ , significant amount of K is also eluted (Fig. 3A). The amount of K eluted  
8 263 previously by  $\text{HNO}_3$  is about the same amount as that was loaded onto the column, so K is not expected  
9 264 during Rb elution with  $\text{NH}_4\text{NO}_3$ . The high K signal during  $\text{NH}_4\text{NO}_3$  elution of Rb is likely caused by K  
10 265 impurities in the  $\text{NH}_4\text{NO}_3$  solution. This is supported by the relatively constant K concentration among all  
11 266 cuts eluted with 4 M  $\text{NH}_4\text{NO}_3$  solution (Fig. 3A). Secondly, we also observed during the tests that the resin  
12 267 was partially dissolved in the  $\text{NH}_4\text{NO}_3$  solution. After passing through the column, the  $\text{NH}_4\text{NO}_3$  solution that  
13 268 contains eluted Rb is clear initially, but small yellow particles form upon heating that could not be re-  
14 269 dissolved. In addition, large amounts of phosphorus and Mo from dissolved AMP are present together with  
15 270 Rb in  $\text{NH}_4\text{NO}_3$ , and they have to be removed before Rb analysis, which requires further purification steps.  
16 271 Converting the eluted Rb from  $\text{NH}_4\text{NO}_3$  solution to  $\text{HNO}_3$  solution is difficult because the decomposition of  
17 272  $\text{NH}_4\text{NO}_3$  by heating can be potentially hazardous since it is a strong oxidizer, and the decomposition  
18 273 reaction is exothermic, which can lead to a runaway reaction under certain conditions.

19 274 To circumvent the problems associated with  $\text{NH}_4\text{NO}_3$ , we additionally tested an elution scheme  
20 275 using HCl and  $\text{NH}_4\text{Cl}$  solutions (Fig. 3B). We lowered the concentration of  $\text{NH}_4\text{Cl}$  to 2.5 M to decrease the  
21 276 K background. For washing out K and matrix elements, we used a mixture of dilute HCl (1 M) and  $\text{NH}_4\text{Cl}$   
22 277 (0.005 M). For eluting Rb, we used a solution of 1 M HCl-2.5 M  $\text{NH}_4\text{Cl}$ . A HCl- $\text{NH}_4\text{Cl}$  mixture instead of a  
23 278 pure  $\text{NH}_4\text{Cl}$  solution was used because the yield of Rb was higher (~80%) with the former than with the  
24 279 latter (~60%). The quite low Rb yield in pure ammonium solutions on the AMP-PAN resin (~60%) is likely  
25 280 caused by partial blocking of the channels in the AMP crystal lattice after Rb fixation (Personal  
26 281 communication with Dr. Šebesta who developed the AMP-PAN resin). A solution to this problem is to use  
27 282 a mixture of HCl- $\text{NH}_4\text{Cl}$  solution for Rb elution, and then to add an additional 10 mL of the 1 M HCl-2.5 M  
28 283  $\text{NH}_4\text{Cl}$  mixture to the column and place it in the oven at 70 °C for batch equilibrium for 2–3 hours, and to  
29 284 repeat this batch equilibration step a second time (Fig. 3B). This treatment partially decomposes the AMP  
30 285 resin and the Rb yield after this treatment is > 95%. While particle formation was observed in the chemistry  
31 286 involving  $\text{NH}_4\text{NO}_3$  solution, no such phenomenon was observed in  $\text{NH}_4\text{Cl}$  elution. This could be because a  
32 287 less concentrated  $\text{NH}_4\text{Cl}$  solution was used (2.5 M  $\text{NH}_4\text{Cl}$  vs. 4 M  $\text{NH}_4\text{NO}_3$ ), and/or the possibility that AMP-  
33 288 PAN is more affected by  $\text{NO}_3^-$ . A virtue of using  $\text{NH}_4\text{Cl}$  is that it is not as hazardous as  $\text{NH}_4\text{NO}_3$  and  
34 289 decomposes into  $\text{NH}_3$  and HCl gas upon heating at a temperature of ~338 °C. In our tests,  $\text{NH}_4\text{Cl}$  was  
35 290 removed from the eluate solution containing the recovered Rb by a two-step heating process: *(i)* the solution  
36 291 was transferred to a Pt crucible (pre-cleaned with double distilled HCl), and evaporated to dryness on a  
37 292 hotplate at a temperature of ~90 °C (at this point  $\text{NH}_4\text{Cl}$  appears as a white solid), and *(ii)* the temperature  
38 293 was slowly increased (to avoid boil over) to around 350 °C on the hotplate, and was held there until all  
39 294  $\text{NH}_4\text{Cl}$  decomposed and no white residue was left. Rubidium left in the Pt crucible was then dissolved in  
40 295 nitric or hydrochloric acid solutions for further treatment.

1  
2  
3 296 The AMP-PAN resin releases large amounts of  $\text{NH}_4^+$ , Mo, and P in the Rb eluate. Although  $\text{NH}_4^+$   
4 297 may be removed (and possibly P as well, given that  $\text{P}_2\text{O}_5$  melts and sublimates at  $\sim 350^\circ\text{C}$ ) during heating of  
5 298 the solution to  $350^\circ\text{C}$ , Mo has to be removed using another resin column. We removed Mo using a 1 mL  
6 299 column (0.8 cm ID and 2 cm length) of 200–400 mesh anion-exchange resin AG1-X8. The complete  
7 300 procedure for extracting Rb using AMP-PAN resin is summarized in Table 1. The Rb blank of the procedure  
8 301 including the elution and the following treatment is  $\sim 80$  ng. We did not consider separating K using the  
9 302 AMP-PAN resin because of the high K background in the ammonium solutions (Fig. 3) and the fact that  
10 303 there are far better alternatives.  
11  
12  
13  
14  
15  
16

### 17 305 3.2 Rubidium and potassium purification using cation-exchange resins

18 306 We performed a series of tests on cation resins, evaluating how resin cross-linkage, acid molarity,  
19 307 column length, pressure drop (flow rate), and temperature affect the separation of Rb and K (Table 2; Figs.  
20 308 4, 5 and 6). The columns used here include both gravity-driven short columns (1.5 cm ID, 6.8 or 9 cm  
21 309 length, and 0.45 cm ID and 20 cm length; Fig. 4), and columns that are extremely long and thin (0.16 cm  
22 310 ID and 70–150 cm in length; Figs. 5 and 6), which were run using the FPLC system and took about 10–40  
23 311 hours for one elution depending on the length and the pressure drop. For gravity-driven columns, about  
24 312 500  $\mu\text{L}$  multi-element solutions (at a concentration for all elements of  $\sim 20$   $\mu\text{g/g}$ ) were loaded onto columns  
25 313 in 0.5 M  $\text{HNO}_3$ , and for the FPLC columns, about 200  $\mu\text{L}$  multi-element solutions were loaded in 0.1 M  
26 314  $\text{HNO}_3$ . The elution of elements was done using 0.5–1 M  $\text{HNO}_3$ . A lower acid molarity is associated with a  
27 315 higher distribution coefficient for cation resins<sup>38,39</sup>, and thus requires a larger amount of eluent. At higher  
28 316 acid molarity, however, the Rb and K elution peaks are less resolved. We used  $\text{HNO}_3$  for the elution instead  
29 317 of  $\text{HCl}$  because the solutions can be directly diluted for MC-ICPMS analyses of concentrations ( $\text{HCl}$  is  
30 318 usually avoided as it produces a wider array of isobaric interferences), but  $\text{HNO}_3$  and  $\text{HCl}$  should yield  
31 319 similar results for cation resins, as the exchanging species of the resin is  $\text{H}^+$ .  
32  
33  
34  
35  
36  
37  
38

39 320 The elution curves are shown in Figs. 4, 5, and 6. Figure 4 shows the test results of gravity-driven  
40 321 columns of cation resin AG 50W-X8 (200–400 mesh), one of the most commonly used cation resins, with  
41 322 column lengths varying from 6.8 to 20 cm (Fig. 4A–C). The effect of pressure drop between column top and  
42 323 bottom was tested using a vacuum box that is commercially available from Eichrom, by setting the pressure  
43 324 drop to 5 psi ( $\sim 0.3$  bar; Fig. 4D). Figure 5 shows test results of the same cation resin, but using longer  
44 325 columns (column length ranging from 70–120 cm), for which the FPLC system was used to pressurize the  
45 326 column head to achieve a reasonable flow rate. Figure 6 shows the test results for a higher cross-linkage  
46 327 cation resin AG 50W-X12 (200–400 mesh) for column lengths of 130 and 150 cm.  
47  
48  
49

50 328 Overall, these elution tests show that: (i) alkali metals (together with Mo and Ti) are eluted out first  
51 329 from the resin by diluted  $\text{HNO}_3$  (ranging from 0.5–1 M in our tests), while major elements such as Fe, Mg,  
52 330 Al, and Ca are bound to the resin until more concentrated acids (6 M  $\text{HNO}_3$  or 6 M  $\text{HCl}$ ) are used. Therefore,  
53 331 alkali metals can be efficiently separated from other elements using cation resins, and (ii) column length,  
54 332 acid molarity, pressure drop (flow rate), temperature, and resin cross-linkage all influence cation resin  
55  
56  
57  
58  
59  
60

1  
2  
3 333 elution. The effects of these parameters are discussed below. An important yet confounding factor,  
4 334 however, is flow rate. According to the theory of plates of chromatography <sup>43</sup>, slow flow rates result in  
5 335 smaller plate heights and better separations. However, if the flow rate is too low, vertical diffusion in the  
6 336 fluid can become important, which can cause the height of the plate to increase <sup>44</sup>. We did not observe this  
7 337 diffusion effect for the columns in this study (*i.e.*, our observation is that a lower flow rate seems always to  
8 338 be associated with a better separation), meaning that even at the lowest flow rates studied, we are not in a  
9 339 regime where vertical diffusion matters. Flow rate, however, is not only dependent on pressure drop, but  
10 340 can change depending on column geometry (length and ID), resin cross-linkage, acid molarity, and  
11 341 temperature. In this study, we did not fully disentangle the effects of flow rate from other parameters, as  
12 342 our final goal was to find an elution scheme that separates Rb, so we focused on those variables that can  
13 343 be explicitly monitored and controlled (*e.g.*, temperature and pressure drop). Nevertheless, the flow rate  
14 344 associated with each elution is also reported.

15 345 For the elution curves, we use resolution  $R$  to define how well two peaks are resolved. The  
16 346 resolution  $R$  is expressed as <sup>45</sup>,

17 347  
18 348 
$$R = \frac{2d}{w_1 + w_2}, \quad (3)$$

19 349  
20 350 where  $d$  is the separation between two peaks, and  $w_1$  and  $w_2$  the widths of the two peaks (*i.e.*, the distance  
21 351 between the points of intersection of the tangents to the inflection points with the base line), and we use  
22 352 the Rb and K peaks in the elution curves to calculate  $R$ .  $d$  and  $w$  are defined in the same unit of mL, so that  
23 353  $R$  is dimensionless. Complete separation of the two peaks is considered to be achieved when  $R > 1$ . We  
24 354 also estimate the number of plates (Table 2) based on the Rb elution peak using <sup>45</sup>,

25 355  
26 356 
$$N = 16 (D/w)^2 = 5.54 (D/w_{0.5})^2, \quad (4)$$

27 357  
28 358 where  $D$  is the volume of the Rb peak maximum, and  $w$  and  $w_{0.5}$  are the width and the width at half height  
29 359 of the Rb peak, respectively. The plate height  $HETP$  can then be calculated from  $N$  and the length of the  
30 360 column  $L$ ,

31 361  
32 362 
$$HETP = L/N. \quad (5)$$

33 363  
34 364 The values of  $N$  and  $HETP$  of the elutions, together with the elution conditions are summarized in Table 2.

35 365 **Column length.** According to the theory of plates for chromatography <sup>43</sup>, longer columns should  
36 366 result in better resolved peaks due to the larger number of theoretical plates. This is clearly observed in our  
37 367 tests of gravity-driven elutions (Fig. 4A–C; Table 2). The gravity-driven AG50W-X8 columns with different  
38 368 lengths of 6.8, 9, and 20 cm (Fig. 4A–C) show a decreasing overlap between elemental peaks ( $R$  increasing  
39 369 from 0.68 to 0.87 to 0.99; corresponding linear flow rates are 0.5, 0.46 and 0.27 cm/min, respectively).

1  
2  
3  
4 370 Although distinguishing the effects between column length and flow rate is difficult, comparing Fig. 4A and  
5 371 B demonstrates that column length is most likely the dominant factor as the flow rates are very similar (0.5  
6 372 vs. 0.46 cm/min).

7  
8 373 AG50W-X8 columns longer than 20 cm were tested using the FPLC system (Fig. 5). We measured  
9 374 elution curves produced by high-pressure (pressure drops of 30 and 60 psi, *i.e.*, ~ 2.1 and 4.1 bar,  
10 375 respectively) FPLC columns with lengths of 70 cm and 120 cm (Fig. 5A–C). The result shows that the 120  
11 376 cm column yields a better separation ( $R = 0.88$ ; flow rate = 4 cm/min) than the 70 cm column ( $R = 0.61$ )  
12 377 with a similar flow rate of 4.6 cm/min. For AG50W-X12 columns, a very similar flow rate was achieved for  
13 378 a 130 and a 150 cm column (Fig. 6A and C), and the 150 cm column shows a better separation ( $R = 1.91$   
14 379 vs. 1.64). However, this could also be partly due to the slightly different acid molarity used for the two  
15 380 columns (0.8 M  $\text{HNO}_3$  vs. 0.7 M  $\text{HNO}_3$ ).

16 381 **Pressure drop (flow rate).** Pressure drop directly controls flow rate. The effect of pressure drop was  
17 382 tested first on short AG50W-X8 columns (Fig. 4C and D). The pressure drop was created by using a vacuum  
18 383 box and was set to be 5 psi (~0.3 bar) (Fig. 4D). Comparing the gravity-driven separation and vacuum box  
19 384 separation using 20 cm-long columns (Fig. 4C and D) shows that the elevated pressure and flow rate (2.1  
20 385 cm/min) lead to wider peaks that overlap significantly with each other ( $R = 0.39$ ) compared to the ambient  
21 386 pressure ( $R = 0.99$ ; flow rate = 0.27 cm/min).

22 387 We also tested the pressure drop on the FPLC long columns. A 70 cm-long column filled with  
23 388 AG50W-X8 resin was run at 30 psi (~2.1 bar; flow rate of 4.6 cm/min) and 60 psi (~4.1 bar; flow rate of 8.3  
24 389 cm/min), respectively (Fig. 5A and B), resulted in a larger overlap between Rb and K peaks ( $R = 0.39$ ) at  
25 390 60 psi than at 30 psi ( $R = 0.62$ ). This suggests again that a higher pressure drop (flow rate) has a negative  
26 391 effect on the separation. Nonetheless, the use of 60 psi is still advantageous because the flow rate was  
27 392 almost doubled compared to 30 psi (*i.e.*, decreasing the elution time by a factor of 2). This is important as  
28 393 the total time for one elution is very long for FPLC columns, ranging from 10 to 40 hours, and only one  
29 394 column can be run at a time. We therefore use 60 psi as the pressure for other tests with the FPLC unit.

30 395 **Acid molarity.** We tested the effect of acid molarity for both AG50W-X8 resin (Fig. 5C and D; 120  
31 396 cm FPLC columns) and AG50W-X12 resin (Fig. 6C and D; 150 cm FPLC columns). For AG50W-X8 resin,  
32 397 two acid molarities of 0.5 and 1 M  $\text{HNO}_3$  were used. Compared to the elution using 0.5 M  $\text{HNO}_3$ , the elution  
33 398 using 1 M  $\text{HNO}_3$  required only half the volume of the 0.5M  $\text{HNO}_3$  to elute the alkali metals. For example,  
34 399 Rb was eluted from the column when ~60 mL 0.5 M  $\text{HNO}_3$  was passed through the column, while the  
35 400 volume was ~30 mL when 1 M  $\text{HNO}_3$  was used. This is consistent with the distribution coefficients reported  
36 401 by Strelow et al.<sup>39</sup> showing that higher acid molarity is associated with lower distribution coefficients. Similar  
37 402 to AG50W-X8 resin, AG50W-X12 resin also shows a decrease in distribution coefficients at higher acid  
38 403 molarity. In terms of alkali metal separation, the 0.5 and 1 M  $\text{HNO}_3$  elutions were broadly similar for the  
39 404 AG50W-X8 resin ( $R = 0.88$  for both, and the flow rates are also similar, ~4 cm/min; Fig. 5C and D). However,  
40 405 the tests with AG50 W-X12 resin showed that a lower acid molarity (0.7 M  $\text{HNO}_3$ ) led to a much better

1  
2  
3  
4 406 separation of Rb from K ( $R = 1.91$ ; Fig. 6C) than the higher acid molarity (1 M  $\text{HNO}_3$ ;  $R = 1.05$ ; Fig. 6D), at  
5 407 similar flow rates of 2.9 and 3.2 cm/min (60 psi or 4.1 bar pressure drop), respectively.

6 408 **Resin cross-linkage.** Previous work on cation resins of X2, X8, and X16 cross-linking suggest that  
7  
8 409 in general the selectivity (resolution) of alkali metals increases with the increase in resin cross-linkage <sup>46</sup>.  
9 410 Here we compare the AG50W-X8 and the AG50W-X12 resin. In general, the AG50W-X12 resin (Fig. 6)  
10 411 resulted in a better separation compared to AG50W-X8 resin (Fig. 5). In the tests done with the AG50W-  
11 412 X8 resin, Rb and K were never completely separated from each other ( $R < 1$ ), and the best separation was  
12 413 achieved using a 120 cm-long column run at 60 psi (4.1 bar) and room temperature ( $R = 0.88$ ; flow rate =  
13 414 4 cm/min; acid molarity = 0.5–1 M; Fig. 5C and D). For the AG 50W-X12 resin, a 130 cm column run under  
14 415 the same pressure drop yielded a complete separation of Rb from K ( $R = 1.64$ ; flow rate = 3 cm/min; acid  
15 416 molarity = 0.8 M; Fig. 6A). The column lengths are slightly different in the two tests (120 cm for AG50W-X8  
16 417 resin *vs.* 130 cm for AG50W-X12 resin), this is because the two columns were made at different times, and  
17 418 the different cross-linkages of the two resins made it difficult to match the exact same length due to their  
18 419 different shrinkage. However, this difference in length is fairly small compared to the total length of the  
19 420 columns (*i.e.*, less than 10% difference), and the effect should be negligible. The acid molarity was also  
20 421 slightly different for the 120cm (1 M  $\text{HNO}_3$ ; Fig. 5C and D) and 130 cm (0.8 M  $\text{HNO}_3$ ; Fig. 6A) columns. As  
21 422 discussed above, the 0.5 M  $\text{HNO}_3$  and 1M  $\text{HNO}_3$  yielded similar results for AG50W-X8 resin ( $R = 0.88$ ; Fig.  
22 423 5C and D). It is thus expected that with an intermediate 0.8 M  $\text{HNO}_3$ , the separation should be similar (*i.e.*,  
23 424  $R$  should be around 0.88) In comparison, the AG 50W-X12 column in 0.8 M resulted in a complete  
24 425 separation between Rb and K ( $R=1.64$ ; Fig. 6A). This suggests that the higher resin cross-linkage helped  
25 426 the separation.

26 427 **Temperature.** The effect of temperature was tested using a 130 cm FPLC column filled with  
27 428 AG50W-X12 resin (Fig. 6A and B). Two elutions at room temperature ( $\sim 20^\circ\text{C}$ ) and  $70^\circ\text{C}$  were performed  
28 429 under a pressure drop of 60 psi (4.1 bar). Temperature can affect several aspects of an elution: (i) it can  
29 430 affect resin/fluid distribution coefficients, (ii) higher temperature promotes faster equilibration between the  
30 431 resin and the eluent, thus lowering the *HETP* and resulting in a better separation, and (iii) higher  
31 432 temperature can accelerate vertical diffusion and thus increase the *HETP* <sup>46</sup>. Our tests showed that the  
32 433 separation of Rb from K at  $70^\circ\text{C}$  ( $R = 0.65$ ) was much worse than that at  $20^\circ\text{C}$  ( $R = 1.64$ ). A possible  
33 434 explanation for such a negative effect of temperature is a faster longitudinal diffusion of elements at higher  
34 435 temperature, resulting in an increase in the *HETP*. Calculation of the *HETP* indeed suggests an increase in  
35 436 the plate height (0.14 cm for  $20^\circ\text{C}$  *vs.* 0.26 cm for  $70^\circ\text{C}$ ; Table 2). However, the flow rates at the two  
36 437 temperatures are quite different, about 3 cm/min at  $20^\circ\text{C}$  and 5.7 cm/min at  $70^\circ\text{C}$ , despite of the same  
37 438 pressure drop of 60 psi (4.1 bar). Therefore, an alternative explanation would be that the difference is mainly  
38 439 caused by the contrast in flow rates. At the current stage, we cannot tell which explanation is correct. We  
39 440 can, however, conclude that increasing temperature does not help with the separation at a fixed pressure,  
40 441 and ambient temperature should be used.

1  
2  
3  
4 442 In summary, our tests show that, (i) longer columns and lower acid molarity result in a better  
5 443 separation, (ii) the higher cross-linkage cation resin AG50W-X12 yields better separations than AG50W-  
6 444 X8, and (iii) faster flow rates associated with higher pressure drop and/or temperature have negative  
7  
8 445 impacts on the separation. Among all the tests on cation-exchange resins AG50W-X8 (Figs. 4 and 5) and  
9 446 AG50W-X12 (Fig. 6), the columns that successfully separated Rb from K were the 130 and 150 cm AG50W-  
10 447 X12 resin columns run at room temperature and a pressure drop of 60 psi (4.1 bar; linear flow rate of ~3  
11 448 cm/min) (Fig. 6A, C, and D), and the best result was achieved with the 150 cm AG50W-X12 resin column  
12 449 using 0.7 M HNO<sub>3</sub> for elution (Fig. 6C).  
13  
14  
15 450

### 16 451 3.3 Rubidium and potassium purification using Sr resin

17  
18 452 The distribution coefficients of alkali metal elements on Sr resin <sup>42</sup> suggest that the largest  
19 453 separation between Rb and K occurs at ~2–3 M HNO<sub>3</sub>. An advantage of using Sr-spec resin for Rb  
20 454 separation is that in 2–3 M HNO<sub>3</sub>, the Sr distribution coefficient is higher than 100 <sup>42</sup>, meaning that it is  
21 455 strongly partitioned onto the resin. Therefore, a low Sr/Rb can be easily achieved in the recovered Rb  
22 456 aliquot. As discussed in Sect. 2.5, a low Sr/Rb ratio is crucial for Rb isotopic analysis because <sup>87</sup>Sr is an  
23 457 isobar of <sup>87</sup>Rb, and a correction of <sup>87</sup>Rb by monitoring <sup>88</sup>Sr is only effective for a <sup>88</sup>Sr/<sup>85</sup>Rb intensity ratio  
24 458 (V/V) lower than 0.001 <sup>14</sup>.  
25  
26  
27

28 459 Using Sr resin to purify Rb was done in two previous studies <sup>14,28</sup>, which used 3 M HNO<sub>3</sub> as the  
29 460 eluent, but with different column lengths. Therefore, we compare how column lengths influence K and Rb  
30 461 separation. About 100 μL of a ~100 μg/g multi-element solution was loaded onto the Sr resin columns of  
31 462 three different lengths (13, 20, and 40 cm, with an ID of 0.45 cm) for measuring elution curves. A vacuum  
32 463 box was used to accelerate the flow rate by setting the pressure drop to 2.5 psi (~0.2 bar). The three  
33 464 columns resulted in different flow rates of 2, 1.5, and 0.8 cm/min, and different resolutions between Rb and  
34 465 K peaks of 1.45, 1.46, and 3.1, respectively (Fig. 7).  
35  
36  
37

38 466 Compared to cation-exchange resins, the Sr resin can separate Rb from K more efficiently, and no  
39 467 overlap between Rb and K peaks was observed for the three column lengths. However, the Rb peak  
40 468 overlaps largely with the peaks of other matrix elements on the 13 and 20 cm column, while the 40 cm  
41 469 column yields better separation of Rb from these elements. Given the overlap between Rb and matrix  
42 470 elements, the Sr resin column could be used as the last clean-up step for Rb and K purification, provided  
43 471 that the matrix elements are removed previously by other columns.  
44  
45  
46  
47 472

## 48 473 4. Discussion

### 49 474 4.1 Comparison between AMP-PAN resin, cation-exchange resins, and Sr resin

50 475 Complete separation of Rb from K is achievable with all three resins (AMP-PAN resin, cation resins,  
51 476 and Sr resins), and the yields for Rb are >95% in all cases. However, all resins have advantages and  
52 477 disadvantages. For AMP-PAN resin, the procedural blank of Rb is very high (~80 ng) compared to the other  
53 478 two procedures using cation-exchange resins (~6 ng) and Sr resin (~0.1 ng). This blank level can be  
54  
55  
56  
57  
58  
59  
60

1  
2  
3  
4 479 problematic if AMP-PAN resin is used to separate Rb from Rb-depleted samples. For example, dissolving  
5 480 ~100 mg lunar mare basalt yields ~100 ng Rb (assuming a Rb concentration of ~1  $\mu\text{g/g}$ ), and 80 ng Rb  
6 481 blank would account for ~45% of total Rb after purification. The high Rb blank is primarily from two sources:  
7 482 ammonium solution ( $\text{NH}_4\text{Cl}$  solution) used for Rb elution, and the AMP-PAN resin itself, which was heated  
8 483 to 70 °C to increase the yield of Rb to >95% by partially decomposing the resin. The high blank may be  
9 484 counterbalanced by using a large amount of material, then the resin capacity needs to be considered. We  
10 485 did not measure the resin capacity for Rb, but previous work have determined the resin capacity for Cs,  
11 486 which is 64 mg Cs  $\text{g}^{-1}$  dry resin <sup>47</sup>. Assuming that Rb and Cs occupy the same sites in the resin, and  
12 487 because they have the same valence, the resin capacity for Cs would translate to ~40 mg Rb  $\text{g}^{-1}$  dry resin.  
13 488 We use 1 mL columns (approximately 0.3 g dry resin), so the column capacity would be ~12 mg Rb. For  
14 489 column chromatography, the loading amount should be much less than the resin capacity to avoid  
15 490 breakthrough. Taking 10% total capacity, one can load about 1 mg Rb, which would translate to ~20 g  
16 491 terrestrial basalts (assuming a 50  $\mu\text{g/g}$  Rb concentration, as in geostandard BCR-1). One would also need  
17 492 to take into account matrix elements occupying resin sites when loading a sample, but overall the resin only  
18 493 has a high selectivity for Rb and Cs and not for matrix elements (Figs. 2 and 3). Therefore, resin capacity  
19 494 does not seem to be a limiting factor for using the resin. Rather, the high blank requires the loaded Rb  
20 495 amount to be high enough so that the blank does not contribute much to the total Rb. To make the  
21 496 contribution of blank less than 10%, the loaded Rb should be higher than 720 ng (*i.e.*,  $80/(80+720)=10\%$ ).

22 497 Rubidium cannot be effectively separated from K using only cation-exchange resins in gravity-  
23 498 driven columns. Overlaps between Rb and K peaks were observed for all gravity-driven columns tested in  
24 499 this study, which have column lengths varying from 6.8 to 20 cm and were filled with AG50W-X8 resin (200–  
25 500 400 mesh). Theoretically, longer columns would result in a better separation, but increasing the column  
26 501 length would decrease the flow rate and lead to a more tedious elution (the elution time of the 20-cm gravity-  
27 502 driven column was ~30 hr). This can be mitigated by increasing the flow rate through a higher pressure  
28 503 drop (using a vacuum box or FPLC) or a higher temperature (using FPLC). Higher flow rates, however,  
29 504 have a negative impact on the separation. Thus, there is a trade-off between column length and flow rate  
30 505 (pressure drop). Complete separation of Rb from K was achieved with 130 and 150 cm columns filled with  
31 506 AG50W-X12 resin, run at a pressure drop of 60 psi (4.1 bar) at room temperature, with a flow rate of 3  
32 507 cm/min (Fig. 6). We took advantage of the FPLC system available in the lab, which can pressurize the top  
33 508 of a column to run long columns, but the FPLC system is not commercially available and therefore the  
34 509 FPLC procedure cannot be easily conducted in other laboratories. Another disadvantage with the long  
35 510 columns is that the elution time is very long, ~40 hours for one complete elution and another 20 hours for  
36 511 cleaning the column. Additionally, only one column can be run through the FPLC unit each time.

37 512 The Sr resin provides the most straightforward way for separating Rb from K among the three  
38 513 resins investigated. The Rb and K peaks were fully separated from each other even with short Sr resin  
39 514 columns (~13 cm in length). The only disadvantage is that the resin is rather expensive and cannot be  
40 515 recycled many times (2- or 3-times re-use is however feasible <sup>28</sup>).

1  
2  
3  
4  
516

## 517 4.2 Complete procedures for Rb and K purification on natural samples

518 Each of the three resins can purify Rb from K, the most difficult part of Rb separation, but they do  
519 not necessarily separate Rb and K from other matrix elements at the same time. In order to separate Rb  
520 and K simultaneously, additional columns are required to remove the matrix elements first. We have  
521 developed three complete chemical procedures using the three different resins to extract Rb (and K) from  
522 rock samples for isotopic analysis by MC-ICPMS. The main motivation for doing so was to assess the  
523 accuracy of Rb isotopic analyses of selected geostandards, which can be used in future studies for ground-  
524 truthing Rb isotopic analyses of samples with unknown compositions. The three procedures are outlined in  
525 Table 1: (i) the AMP-PAN resin method includes a first column using AMP-PAN resin to separate Rb from  
526 K and other matrix elements, followed by a second anion-exchange resin AG1-X8 column to remove Mo in  
527 the Rb eluent that comes from the AMP-PAN resin, (ii) the cation-exchange resins + FPLC method uses  
528 three columns. The first is a gravity-driven AG50W-X8 column that is used to separate Rb and K from matrix  
529 elements, the second is an anion-exchange resin column to remove Ti whose elution peak overlaps with K  
530 and Rb peaks in the previous step, and the third is a FPLC long column of 150 cm length filled with AG50W-  
531 X12 resin to quantitatively separate Rb and K from each other, and (iii) the Sr resin method follows Nie and  
532 Dauphas<sup>14</sup>, which uses first a column filled with cation-exchange resin AG50W-X8 to separate Rb and K  
533 from matrix elements, followed by a column of anion-exchange resin AG1-X8 to further purify Rb and K by  
534 removing matrix element Ti, then followed by a Sr resin column to separate Rb and K from each other. All  
535 three methods completely separate Rb from K, and for methods (ii) and (iii), K was purified at the same  
536 time (both methods quantitatively recover K with a low K blank of less than 20 ng), and can be used for K  
537 isotopic analysis.

538

## 539 4.3 Applications to synthetic and natural samples

540 We tested the reliability of the three Rb purification methods in the determination of Rb isotopic  
541 compositions by MC-ICPMS using natural and synthetic samples. The samples (Table 3) include the Rb  
542 isotopic reference standard SRM984 and several geostandards. The geostandards comprised three basalts  
543 (BCR-2, BHVO-2, BE-N), one andesite (AGV-2), and three granites (GS-N, G-3, G-A). Additionally, we  
544 doped two Rb-depleted (Rb concentration of ~0.5 µg/g) peridotite/dunite geostandards (PCC-1/DTS-2b)  
545 with the SRM984 solution to produce a mixture in which less than 1% of the total Rb derives from the rocks.  
546 The rationale for this was to process samples with a known Rb isotopic composition but with chemical  
547 compositions of natural rocks.

548 We digested these samples in various mixtures of HF-HNO<sub>3</sub>-HCl-HClO<sub>4</sub> acids, following the  
549 protocol used by Nie and Dauphas<sup>14</sup>. Briefly, the samples were first dissolved in a mixture of concentrated  
550 HF-HNO<sub>3</sub> (2:1 in volume) with a few drops of HClO<sub>4</sub> on a hotplate at 130 °C. The sample solutions were  
551 then dried at ~170 °C (for evaporating HClO<sub>4</sub>), re-dissolved in aqua regia (3:1 volume mixture of  
552 concentrated HCl-HNO<sub>3</sub>) at 130 °C for another 24 hr. After repeating the aqua regia step for a second time,

1  
2  
3 553 the samples were re-dissolved in sample loading media for columns. We separated Rb from these samples  
4 554 using the three methods above (Table 1) and measured the Rb isotopic compositions using MC-ICPMS.  
5 555 The obtained Rb isotopic compositions of the samples are reported in Table 3. The  $\delta^{87}\text{Rb}$  values of the  
6 556 geostandards agree well with the values reported previously<sup>12,14,28</sup>. For the samples that were purified using  
7 557 more than one Rb separation method from this study, the  $\delta^{87}\text{Rb}$  values are compared in Fig. 8. We applied  
8 558 the AMP-PAN method to only Rb-enriched samples of synthetic ones and granites because of its high Rb  
9 559 blank (~80 ng), but the tests of the cation-exchange resins + FPLC method and the Sr resin method (with  
10 560 Rb blank levels of ~6 and ~0.1 ng, respectively) were extended to also relatively low-Rb andesites and  
11 561 basalts. The three methods produced  $\delta^{87}\text{Rb}$  values that agree within uncertainties (Fig. 8).

12 562 The high-blank problem of AMP-PAN resin could be alleviated by increasing the sample mass  
13 563 processed with chromatography chemistry. Terrestrial crust is enriched in Rb because alkali elements are  
14 564 incompatible during magmatic differentiation, but samples from other planetary bodies (*e.g.*, lunar samples  
15 565 and chondrites) have Rb concentrations by a factor of ~100 lower. Therefore, despite the fact that the AMP-  
16 566 PAN resin can separate Rb from K efficiently with only a small 1 mL resin column, the method might only  
17 567 be suitable for high-Rb terrestrial samples. In contrast, the cation-exchange resins + FPLC method and the  
18 568 Sr resin method do not have blank issues and can be applied to Rb-depleted samples. The latter two  
19 569 methods also separate K simultaneously, whose isotopic composition can be measured by MC-ICPMS. As  
20 570 discussed above, however, the cation-exchange resins + FPLC method would require a FPLC system that  
21 571 is not commercially available. Therefore, the Sr resin method is the most efficient and easily implementable  
22 572 method to separate both Rb and K for isotopic analysis of these two elements.

23 573  
24 574

## 25 575 Conclusion

26 576 We tested the effectiveness of three types of resins that have been used to purify Rb from K and  
27 577 matrix elements prior to isotopic analysis by MC-ICPMS, including AMP-PAN resin, cation-exchange resins,  
28 578 and Sr resin. We find that the AMP-PAN resin is highly effective in separating Rb from K and other matrix  
29 579 elements, but it has a high Rb blank (~80 ng) and is tedious to implement.

30 580 We tested the effect of column length, acid molarity, temperature, pressure drop (flow rate), and  
31 581 resin cross-linkage on Rb and K separation using cation-exchange resins. Increasing column length helps  
32 582 the separation, while increasing acid molarity, temperature, or pressure drop (flow rates) has negative  
33 583 impacts on the separation. Complete separation of Rb from K was not achieved using gravity-driven  
34 584 AG50W-X8 columns with column lengths ranging from 6.8 cm to 20 cm. Increasing column length and resin  
35 585 cross-linkage from AG50W-X8 to AG50W-X12 have positive effects on the separation. Complete  
36 586 separation of Rb from K was achieved using AG50W-X12 resin filled in a column of 0.16 cm inner diameter  
37 587 and 150 cm length installed in a FPLC system, run at room temperature and a flow rate of 3 cm/min (60 psi  
38 588 or 4.1 bar pressure drop). The Rb blank of the procedure using cation resins to purify Rb is ~6 ng.

1  
2  
3 589 The Sr resin can cleanly and efficiently separate Rb from K, and a relatively short column (13–40  
4 590 cm in length) is sufficient. The Rb blank of the separation procedure using this resin is only ~0.1 ng.  
5  
6 591 Therefore, Sr resin is the optimal choice among the three resins to separate Rb from K.  
7

8 592 Three chemical procedures for the separation of Rb from natural samples using the three resins  
9 593 were designed (Table 1), and tested with synthetic solutions and natural rocks. We measured the Rb  
10 594 isotopic compositions of purified Rb solutions from those tests using MC-ICPMS. The three procedures  
11 595 yielded consistent Rb isotopic compositions. The cation-exchange resins + FPLC procedure and the Sr  
12 596 resin procedure allow purification of both Rb and K from single digestion aliquots, and can be applied to a  
13 597 large variety of terrestrial and meteorite samples for combined Rb and K isotopic studies.  
14  
15  
16 598  
17  
18  
19  
20  
21  
22  
23  
24  
25  
26  
27  
28  
29  
30  
31  
32  
33  
34  
35  
36  
37  
38  
39  
40  
41  
42  
43  
44  
45  
46  
47  
48  
49  
50  
51  
52  
53  
54  
55  
56  
57  
58  
59  
60

**Acknowledgments**

This work was supported by a NASA NESSF fellowship (NNX15AQ97H), a Carnegie postdoctoral fellowship, and a Carnegie Postdoc × Postdoc (P<sup>2</sup>) seed grant to NXN, NASA grants NNX17AE86G, NNX17AE87G, 80NSSC17K0744, 80NSSC20K0821, and NSF grant EAR-2001098 to ND.

## References

- 1 E. L. Garner, L. A. Machlan and I. L. Barnes, in *Lunar and Planetary Science Conference Proceedings*, 1975, vol. 6, pp. 1845–1855.
- 2 M. Humayun and R. N. Clayton, *Geochimica et Cosmochimica Acta*, 1995, **59**, 2115–2130.
- 3 C. M. O. Alexander, J. N. Grossman, J. Wang, B. Zanda, M. Bourot-Denise and R. H. Hewins, *Meteoritics & Planetary Science*, 2000, **35**, 859–868.
- 4 J. S. Pistiner and G. M. Henderson, *Earth and Planetary Science Letters*, 2003, **214**, 327–339.
- 5 C. M. O. Alexander and J. N. Grossman, *Meteoritics & Planetary Science*, 2005, **40**, 541–556.
- 6 O. Nebel, K. Mezger and W. van Westrenen, *Earth and planetary science letters*, 2011, **305**, 309–316.
- 7 S. Misra and P. N. Froelich, *Science*, 2012, **335**, 818–823.
- 8 P. A. P. Von Strandmann, H. C. Jenkyns and R. G. Woodfine, *Nature Geoscience*, 2013, **6**, 668–672.
- 9 P. B. Tomascak, T. Magna and R. Dohmen, *Advances in lithium isotope geochemistry*, Springer, 2016.
- 10 K. Wang and S. B. Jacobsen, *Nature*, 2016, **538**, 487–490.
- 11 S. Penniston-Dorland, X.-M. Liu and R. L. Rudnick, *Reviews in Mineralogy and Geochemistry*, 2017, **82**, 165–217.
- 12 E. A. Pringle and F. Moynier, *Earth and Planetary Science Letters*, 2017, **473**, 62–70.
- 13 S. Li, W. Li, B. L. Beard, M. E. Raymo, X. Wang, Y. Chen and J. Chen, *PNAS*, 2019, **116**, 8740–8745.
- 14 N. X. Nie and N. Dauphas, *ApJL*, 2019, **884**, L48.
- 15 H. D. Hanna, X.-M. Liu, Y.-R. Park, S. M. Kay and R. L. Rudnick, *Geochimica et Cosmochimica Acta*, 2020, **278**, 322–339.
- 16 Y. Hu, F.-Z. Teng, T. Plank and C. Chauvel, *Science advances*, 2020, **6**, eabb2472.
- 17 P. Koefoed, O. Pravdivtseva, H. Chen, C. Gerritzen, M. M. Thiemens and K. Wang, *Meteoritics & Planetary Science*, DOI:https://doi.org/10.1111/maps.13545.
- 18 H. Bloom, K. Lodders, H. Chen, C. Zhao, Z. Tian, P. Koefoed, M. K. Pető, Y. Jiang and K. Wang (王昆), *Geochimica et Cosmochimica Acta*, 2020, **277**, 111–131.
- 19 Y. Jiang, P. Koefoed, O. Pravdivtseva, H. Chen, C.-H. Li, F. Huang, L.-P. Qin, J. Liu and K. Wang, *Meteoritics & Planetary Science*, 2021, **56**, 61–76.
- 20 Y. Hu, F.-Z. Teng and C. Chauvel, *Geochimica et Cosmochimica Acta*, 2021, **295**, 98–111.
- 21 Z. J. Zhang, N. X. Nie, R. A. Mendybaev, M.-C. Liu, J. J. Hu, T. Hopp, E. E. Alp, B. Lavina, E. S. Bullock and K. D. McKeegan, *ACS Earth and Space Chemistry*.
- 22 K. Wang (王昆) and S. B. Jacobsen, *Geochimica et Cosmochimica Acta*, 2016, **178**, 223–232.
- 23 W. Li, X.-M. Liu and L. V. Godfrey, *Geostandards and Geoanalytical Research*, 2019, **43**, 261–276.
- 24 G. Zhu, J. Ma, G. Wei and L. Zhang, *Frontiers in Chemistry*.
- 25 K. S. Heier and J. A. Adams, *Physics and Chemistry of the Earth*, 1964, **5**, 253–381.
- 26 Y. Hu, X.-Y. Chen, Y.-K. Xu and F.-Z. Teng, *Chemical Geology*, 2018, **493**, 100–108.
- 27 J. F. Rudge, B. C. Reynolds and B. Bourdon, *Chemical Geology*, 2009, **265**, 420–431.

- 1  
2  
3 28 Z. Zhang, J. Ma, L. Zhang, Y. Liu and G. Wei, *Journal of Analytical Atomic Spectrometry*, 2018, **33**, 322–  
4 328.  
5  
6 29 T. Waight, J. Baker and B. Willigers, *Chemical Geology*, 2002, **186**, 99–116.  
7  
8 30 O. Nebel, K. Mezger, E. Scherer and C. Münker, *International Journal of Mass Spectrometry*, 2005, **246**,  
9 10–18.  
10  
11 31 H. Zeng, V. F. Rozsa, N. X. Nie, Z. Zhang, T. A. Pham, G. Galli and N. Dauphas, *ACS Earth Space*  
12 *Chem.*, 2019, **3**, 2601–2612.  
13  
14 32 J. van R. Smit, W. Robb and J. J. Jacobs, *Journal of Inorganic and Nuclear Chemistry*, 1959, **12**, 104–  
15 112.  
16  
17 33 C. J. Coetzee, *Journal of Chemical Education*, 1972, **49**, 33.  
18  
19 34 J. van R. Smit, J. J. Jacobs and W. Robb, *Journal of Inorganic and Nuclear Chemistry*, 1959, **12**, 95–  
20 103.  
21  
22 35 K. Brewer, T. Todd, D. Wood, P. Tullock, F. Sebesta, J. John and A. Motl, *Czechoslovak journal of*  
23 *physics*, 1999, **49**, 959–964.  
24  
25 36 T. J. Ireland, F. L. H. Tissot, R. Yokochi and N. Dauphas, *Chemical Geology*, 2013, **357**, 203–214.  
26  
27 37 H. Li, F. L. Tissot, S.-G. Lee, E. Hyung and N. Dauphas, *ACS Earth and Space Chemistry*, 2020, **5**, 55–  
28 65.  
29  
30 38 F. W. E. Strelow, *Analytical Chemistry*, 1960, **32**, 1185–1188.  
31  
32 39 F. W. Strelow, R. Rethemeyer and C. J. C. Bothma, *Analytical Chemistry*, 1965, **37**, 106–111.  
33  
34 40 United States, US20150008171A1, 2015.  
35  
36 41 J. Y. Hu, N. Dauphas, F. L. H. Tissot, R. Yokochi, T. J. Ireland, Z. Zhang, A. M. Davis, F. J. Ciesla, L.  
37 Grossman, B. L. A. Charlier, M. Roskosz, E. E. Alp, M. Y. Hu and J. Zhao, *Sci. Adv.*, 2021, **7**, eabc2962.  
38  
39 42 E. Philip Horwitz, R. Chiarizia and M. L. Dietz, *Solvent extraction and ion exchange*, 1992, **10**, 313–336.  
40  
41 43 A. J. Martin and R. L. Synge, *Biochemical Journal*, 1941, **35**, 1358–1368.  
42  
43 44 J. J. van Deemter, F. J. Zuiderweg and A. Klinkenberg, *Chemical Engineering Science*, 1956, **5**, 271–  
44 289.  
45  
46 45 L. R. Snyder, J. J. Kirkland and J. W. Dolan, *Introduction to modern liquid chromatography*, John Wiley  
47 & Sons, 2011.  
48  
49 46 R. Dybczyński, *Journal of Chromatography A*, 1972, **72**, 507–522.  
50  
51 47 R. S. Herbst, J. D. Law, T. A. Todd, D. Wood, T. G. Garn and E. L. Wade, *Integrated AMP-PAN, TRUEX,*  
52 *and SREX flowsheet test to remove cesium, surrogate actinide elements, and strontium from INEEL*  
53 *tank waste using sorbent columns and centrifugal contactors*, Idaho National Laboratory (INL), 2000.  
54  
55  
56  
57  
58  
59  
60

Table 1. Elution sequences of the three Rb purification procedures.

Separation steps	Reagents	Volume (mL)	Comments
<b>1) AMP-PAN resin method</b>			
<i>Column 1, AMP-PAN resin, 1 mL resin (0.8 cm ID, 2 cm length) in Bio-Rad Poly-Prep columns</i>			
Conditioning	1 M HCl - 0.005 M NH <sub>4</sub> Cl	2	
Sample loading	1 M HCl - 0.005 M NH <sub>4</sub> Cl	0.1	
Elution of K and matrix elements	1 M HCl - 0.005 M NH <sub>4</sub> Cl	20	
Elution of Rb	1 M HCl - 1 M NH <sub>4</sub> Cl	20	
Further recovery of Rb from resin	1 M HCl - 2.5 M NH <sub>4</sub> Cl	10	Batch extraction at 70 °C
Further recovery of Rb from resin	1 M HCl - 2.5 M NH <sub>4</sub> Cl	10	Batch extraction at 70 °C
Combine and dry the recovered Rb solutions in Pt crucible at 350 °C			Removal of NH <sub>4</sub> Cl
<i>Column 2, AG1-X8 resin, 200–400 mesh, 1 mL resin (0.8 cm ID, 2 cm length) in Bio-Rad Poly-Prep columns</i>			
			For Mo removal
Conditioning	5 M HCl - H <sub>2</sub> O <sub>2</sub>	2	H <sub>2</sub> O <sub>2</sub> / HCl = 0.5 % (v/v)
Sample loading	5 M HCl - H <sub>2</sub> O <sub>2</sub>	1	H <sub>2</sub> O <sub>2</sub> / HCl = 0.5 % (v/v)
Elution of Rb	5 M HCl	9	Mo stays on the column
<b>2) Cation-exchange resins + FPLC method</b>			
<i>Column 1, AG50W-X8 resin, 200–400 mesh, 16 mL resin (1.5 cm ID, 9 cm length) in Bio-Rad Econo-Pac columns</i>			
Conditioning	0.5 M HNO <sub>3</sub>	16	
Sample loading	0.5 M HNO <sub>3</sub>	≤8	
Elution of matrix	0.5 M HNO <sub>3</sub>	130	
Elution of Rb and K	0.5 M HNO <sub>3</sub>	350*	Contains some Ti
<i>Column 2, AG1-X8 resin, 200–400 mesh, 1 mL resin (0.8 cm ID, 2 cm length) in Bio-Rad Poly-Prep columns</i>			
			For Ti removal
Conditioning	2 M HF	2	
Sample loading	2 M HF	0.25	
Elution of Rb and K	2 M HF	9	Ti stays on the column
<i>Column 3, AG50W-X12 resin, 200–400 mesh, home-made column of 0.16 cm ID and 150 cm length on FPLC</i>			
			Elution at pressure drop of 60 psi (linear flow rate of ~3 cm/min)
Conditioning	0.1 M HNO <sub>3</sub>	10	
Sample loading	0.1 M HNO <sub>3</sub>	0.2	
Elution of K	0.7 M HNO <sub>3</sub>	~85 <sup>†</sup>	
Elution of Rb	0.7 M HNO <sub>3</sub>	~35 <sup>†</sup>	
<b>3) Sr resin method</b>			
<i>Column 1, AG50W-X8 resin, 200–400 mesh, 16 mL resin (1.5 cm ID, 9 cm length) in Bio-Rad Econo-Pac columns</i>			
Conditioning	0.5 M HNO <sub>3</sub>	16	
Sample loading	0.5 M HNO <sub>3</sub>	≤8	

1				
2				
3	Elution of matrix	0.5 M HNO <sub>3</sub>	130	
4	Elution of K and Rb	0.5 M HNO <sub>3</sub>	350*	Contains some Ti
5	<hr/>			
6	<b>Column 2, AG1-X8 resin, 200–400 mesh, 1 mL resin (0.8 cm ID, 2 cm length) in Bio-Rad</b>			
7	<b>Poly-Prep columns</b>			For Ti removal
8				
9	Conditioning	2 M HF	2	
10	Sample loading	2 M HF	0.25	
11	Elution of Rb and K	2 M HF	9	Ti stays on the column
12	<hr/>			
13	<b>Column 3, Sr resin, 50–100 μm size, in Savillex columns of 0.45 cm ID and 40 cm length</b>			Elution at pressure drop of
14				2.5 psi (linear flow rate of
15	Conditioning	3 M HNO <sub>3</sub>	5	0.8 cm/min)
16				
17	Sample loading	3 M HNO <sub>3</sub>	0.1	
18	Elution of matrix	3 M HNO <sub>3</sub>	3.9	
19	Elution of Rb	3 M HNO <sub>3</sub>	12	
20	Elution of K	3 M HNO <sub>3</sub>	20	
21	<hr/>			

22 \*The 350 mL eluate solutions were collected using Savillex PFA jars of 360 mL volume, dried on a hotplate at 130 °C,  
 23 and re-dissolved in HF for the following step. †Eluate was collected every 1 mL between 80 and 90 mL elution, and Rb  
 24 and K concentrations were measured in each collected volume to decide on the cutoff between Rb and K peaks. The  
 25 collected volumes were then consolidated into K and Rb solutions. ID: inner diameter. v/v: volume/volume.  
 26  
 27  
 28  
 29  
 30  
 31  
 32  
 33  
 34  
 35  
 36  
 37  
 38  
 39  
 40  
 41  
 42  
 43  
 44  
 45  
 46  
 47  
 48  
 49  
 50  
 51  
 52  
 53  
 54  
 55  
 56  
 57  
 58  
 59  
 60

Table 2. Conditions of the elutions using cation-exchange resins.

Elution	Resin type	Column length (cm)	Column ID (cm)	Temperature (°C)	Pressure drop (psi)*	HNO <sub>3</sub> molarity	Linear flow rate (cm/min)	Number of plates <sup>#</sup>	Height of plate (cm)	Resolution <sup>†</sup>
Fig. 3A	AG50W-X8	6.8	1.5	20	0	0.5	0.50	232	0.03	0.68
Fig. 3B	AG50W-X8	9	1.5	20	0	0.5	0.46	322	0.03	0.87
Fig. 3C	AG50W-X8	20	0.45	20	0	0.5	0.27	360	0.06	0.99
Fig. 3D	AG50W-X8	20	0.45	20	5	0.5	2.11	56	0.36	0.43
Fig. 4A	AG50W-X8	70	0.16	20	30	0.5	4.61	280	0.25	0.61
Fig. 4B	AG50W-X8	70	0.16	20	60	0.5	8.30	185	0.38	0.39
Fig. 4C	AG50W-X8	120	0.16	20	60	0.5	4.00	357	0.34	0.88
Fig. 4D	AG50W-X8	120	0.16	20	60	1	3.91	549	0.22	0.88
Fig. 5A	AG50W-X12	130	0.16	20	60	0.8	2.99	902	0.14	1.64
Fig. 5B	AG50W-X12	130	0.16	70	60	0.8	5.72	507	0.26	0.65
Fig. 5C	AG50W-X12	150	0.16	20	60	0.7	2.93	1007	0.15	1.91
Fig. 5D	AG50W-X12	150	0.16	20	60	1	3.21	466	0.32	1.05

\*Pressure drop is in psi. 5, 30 and 60 psi are equivalent to ~0.34, 2.06 and 4.14 bar, respectively. <sup>#</sup>Number of plates is estimated based on Rb peaks using  $N = 16 (D/w)^2$ , where D is the volume corresponding to the elution of the Rb peak and w is the width of the Rb peak. <sup>†</sup>Resolution is calculated based on the separation between Rb and K peaks. ID: inner diameter.

Table 3. Rubidium isotopic compositions of geostandards and synthetic samples using the three

Samples	Rock type	$\delta^{87}\text{Rb}$ (‰) <sub>SRM984</sub>	95 % c.i.	n <sup>†</sup>
<b>1) AMP-PAN resin method (Rb blank of ~80 ng, Rb yield &gt;95%)</b>				
SRM984	Reference standard	-0.02	0.03	10
SRM984 + PCC-1(I)*	Mixture of reference standard and Rb-depleted peridotite	-0.02	0.03	10
SRM984 + PCC-1(II)*	Mixture of reference standard and Rb-depleted peridotite	-0.05	0.03	10
GS-N	Granite	-0.20	0.03	10
G-3	Granite	-0.28	0.03	10
<b>2) Cation-exchange resins + FPLC (Rb blank of ~6 ng, Rb yield &gt;95%)</b>				
SRM984	Reference standard	0.03	0.03	9
SRM984 + DTS-2b	Mixture of reference standard and Rb-depleted dunite	-0.02	0.03	7
BCR-2 (I)*	Basalt	-0.16	0.01	9
BCR-2 (II)*	Basalt	-0.15	0.01	9
BHVO-2	Basalt	-0.11	0.01	9
BE-N	Basalt	-0.10	0.02	9
AGV-2	Andesite	-0.13	0.02	9
GS-N	Granite	-0.14	0.05	8
G-3	Granite	-0.24	0.01	9
G-A	Granite	-0.22	0.03	9
<b>3) Sr resin method (Rb blank of ~0.1 ng, Rb yield &gt;95%)</b>				
SRM984 + PCC-1	Mixture of reference standard and Rb-depleted peridotite	-0.02	0.04	9
BCR-2	Basalt	-0.16	0.02	9
BHVO-2	Basalt	-0.12	0.02	9
AGV-2	Andesite	-0.15	0.02	9
GS-N	Granite	-0.19	0.02	9
G-3	Granite	-0.23	0.03	7

different purification procedures in Table 1.

\* (I) and (II) denote different digestions.  $\delta^{87}\text{Rb}$  is defined as:  $\delta^{87}\text{Rb} = [(^{87}\text{Rb}/^{85}\text{Rb})_{\text{sample}} / (^{87}\text{Rb}/^{85}\text{Rb})_{\text{SRM984}} - 1] \times 1000$ .

<sup>†</sup>n is the number of replicate analyses.

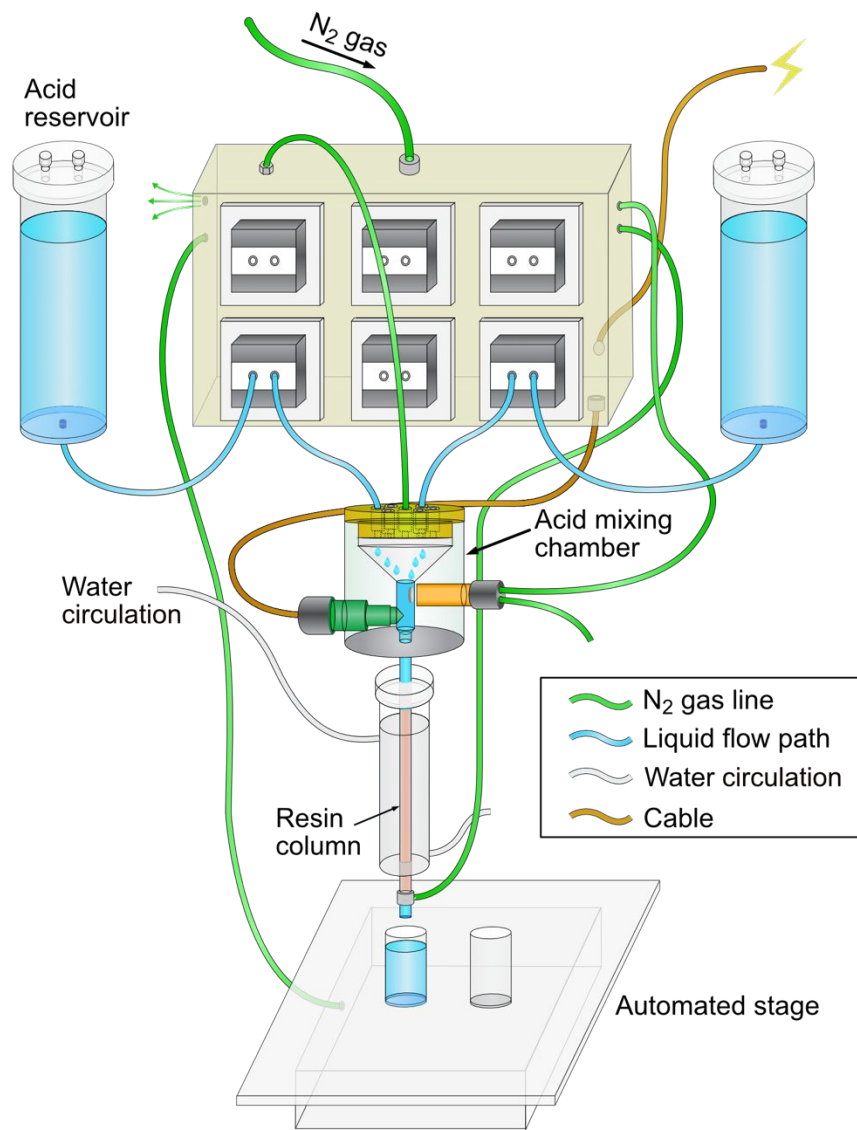


Fig. 1. The sketch of the fluoropolymer pneumatic liquid chromatography (FPLC) system. The major components of the system include acid reservoirs (filled with acids in different molarities and Milli-Q water), acid mixing chamber (to obtain acids in different molarities by mixing with Milli-Q water), the resin column, and the stage that is automatically movable for collecting eluents in different vials. The system is automated and computer-controlled using a LabView software interface. Elution pressure is adjustable (from 0 to 70 psi, *i.e.*, 4.8 bar) by pressurizing

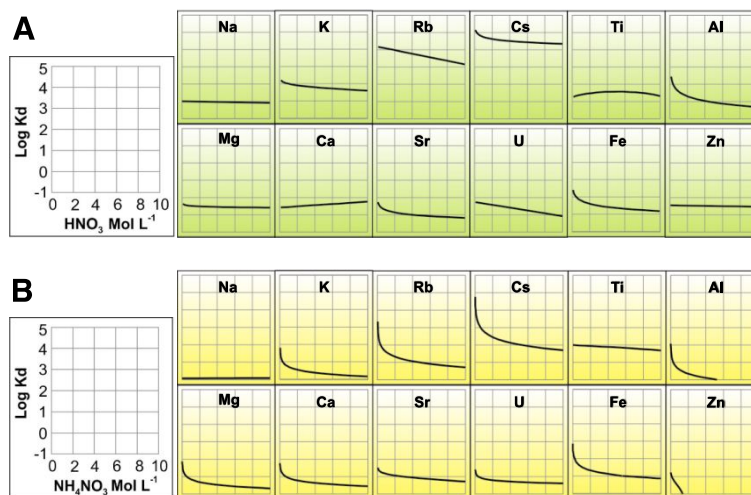


Fig. 2. Distribution coefficients ( $K_d$ ) in base-10 logarithmic scale of alkali metal elements and several other elements on AMP-PAN resin, as a function of (A)  $\text{HNO}_3$  molarity, and (B)  $\text{NH}_4\text{NO}_3$

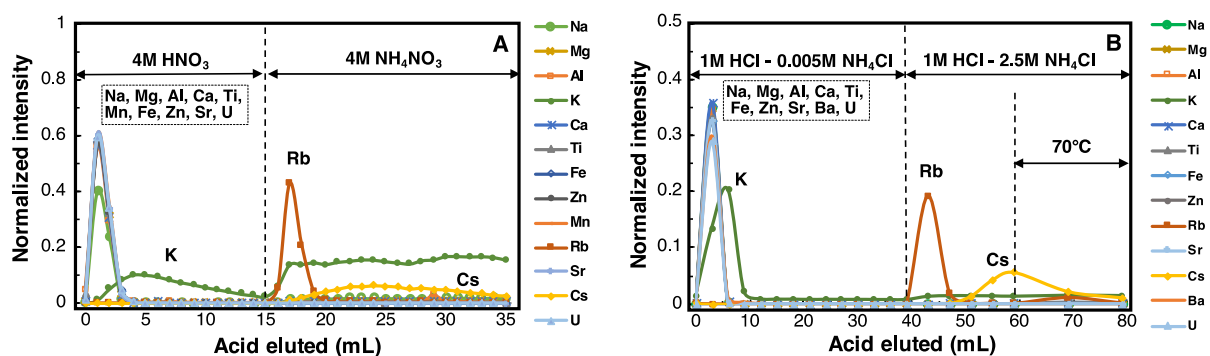


Fig. 3. Elution curves of elements on AMP-PAN resin. (A) Elution using HNO<sub>3</sub> and NH<sub>4</sub>NO<sub>3</sub>. Several problems have been observed for this elution scheme, including resin decomposition during elution, high K blank in NH<sub>4</sub>NO<sub>3</sub>, and difficulties in follow-up treatment of the Rb in NH<sub>4</sub>NO<sub>3</sub> eluate (see Sect. 3.1 for details). (B) Purification of Rb with AMP-PAN resin using HCl and NH<sub>4</sub>Cl. Rubidium was eluted in two steps. A solution of 1 M HCl - 2.5 M NH<sub>4</sub>Cl was first passed through the resin to collect Rb (~70–80 % of the total Rb was recovered) and the

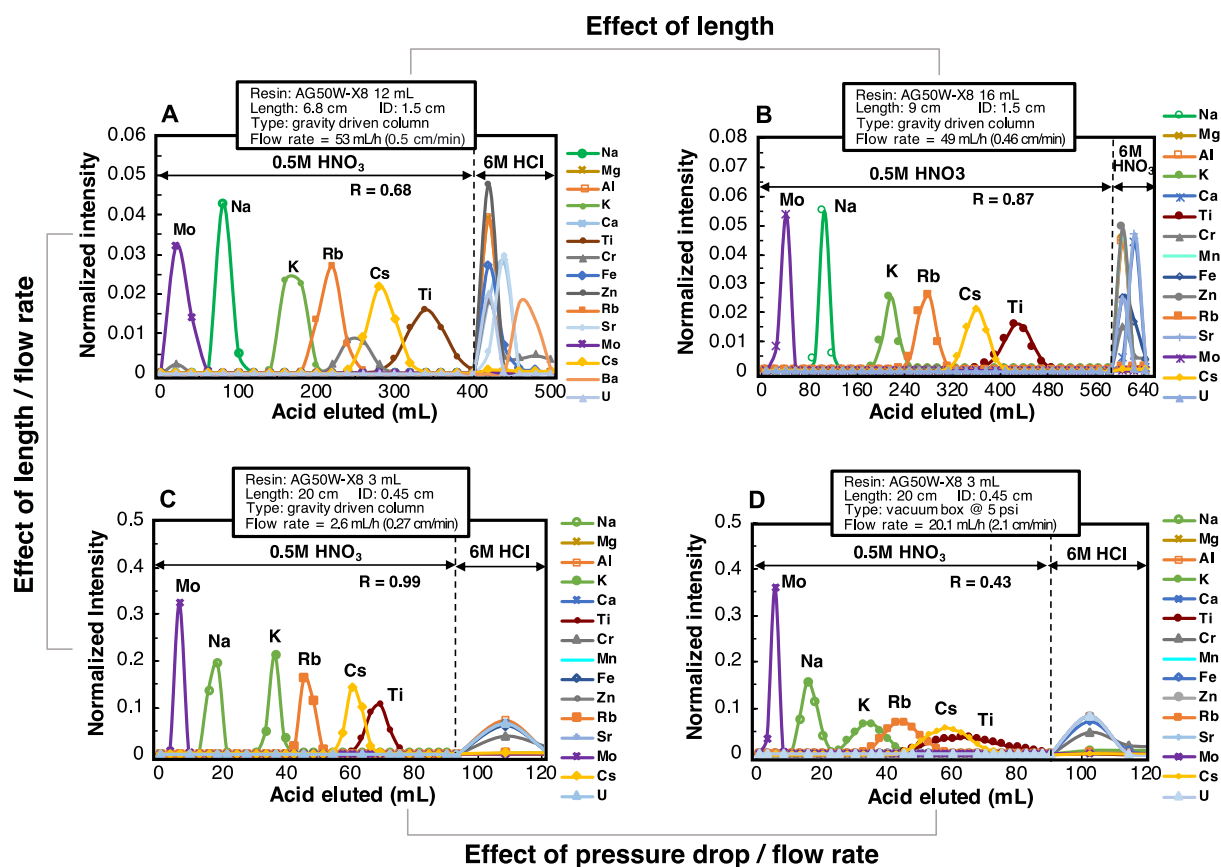


Fig. 4. Elution curves of gravity-driven AG50W-X8 (200–400 mesh) resin columns and of a column under slight pressurization (pressure drop of 5 psi or ~0.3 bar). Different lengths were

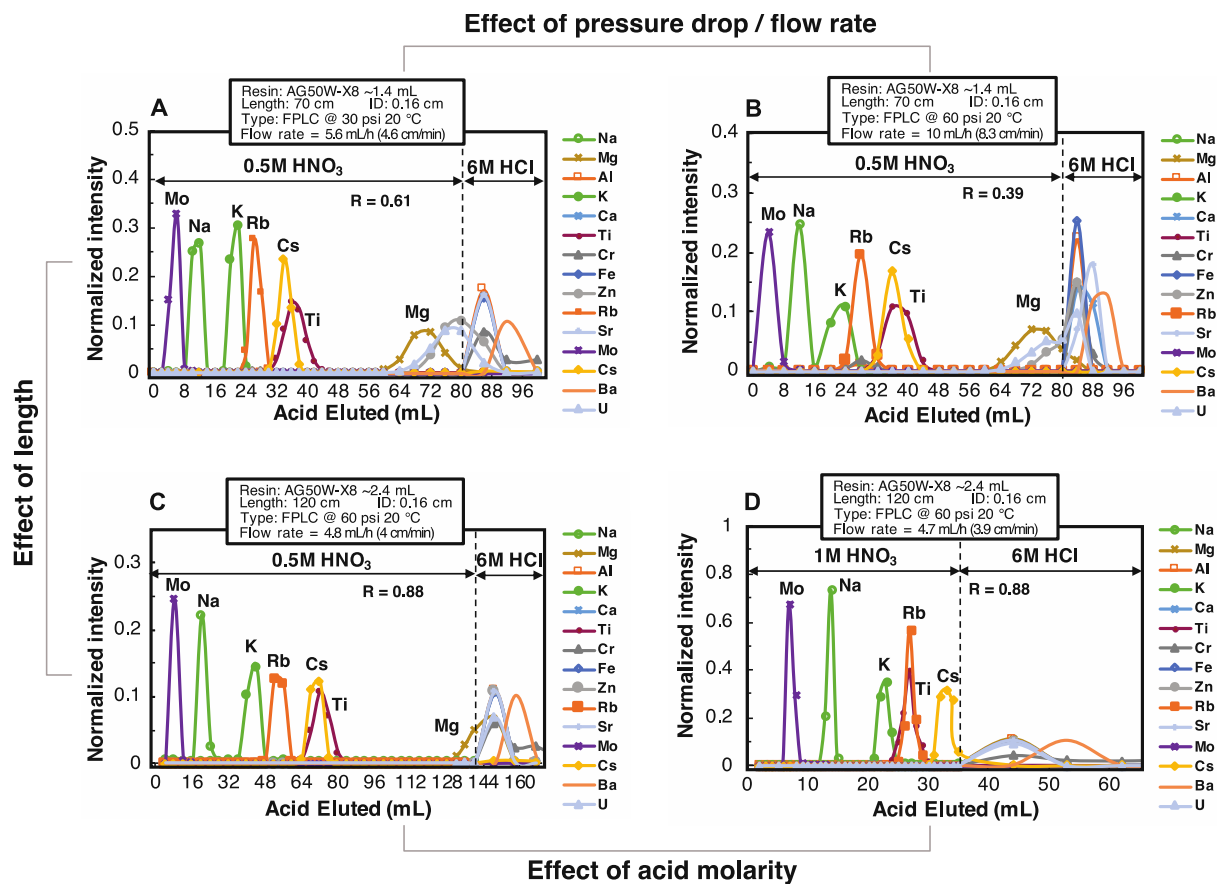


Fig. 5. Elution curves of AG50W-X8 (200–400 mesh) resin columns, obtained at different

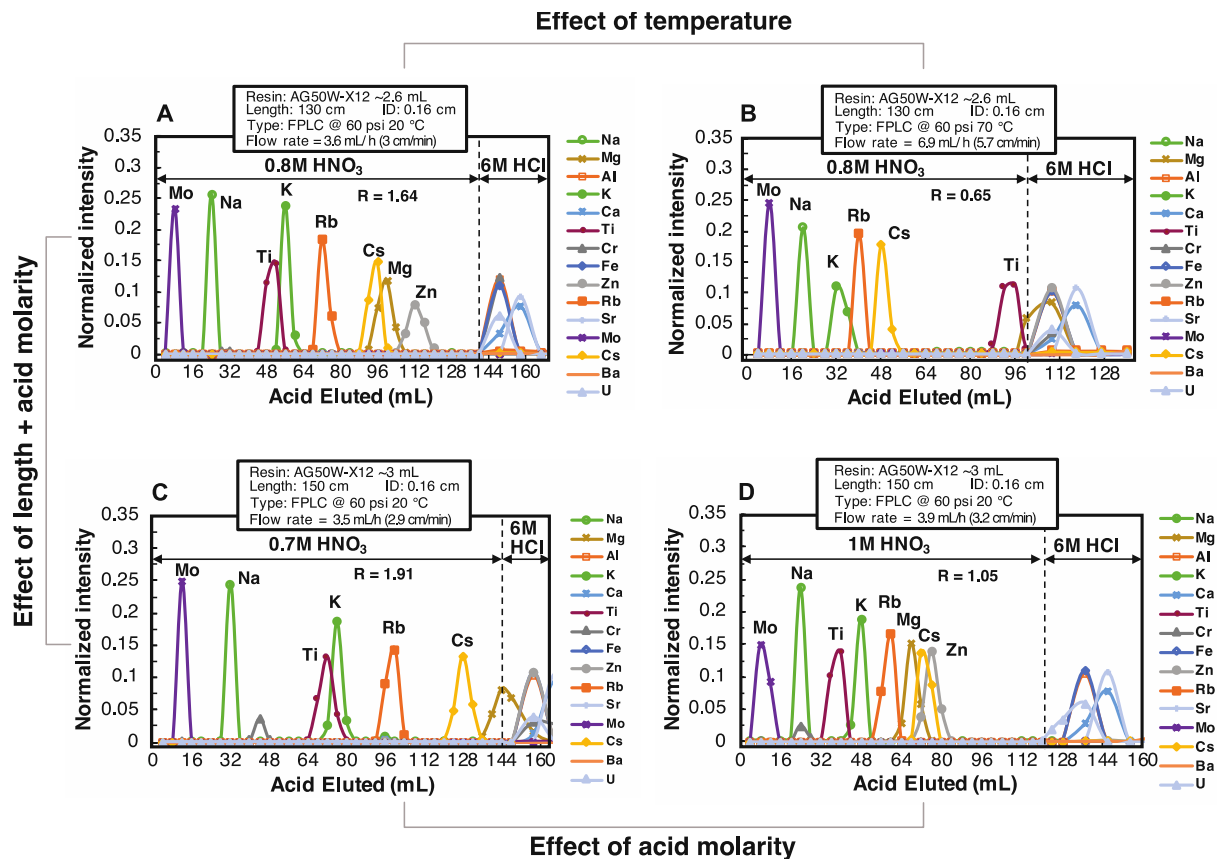


Fig. 6. Elution curves of AG50W-X12 (200–400 mesh) resin columns tested at different

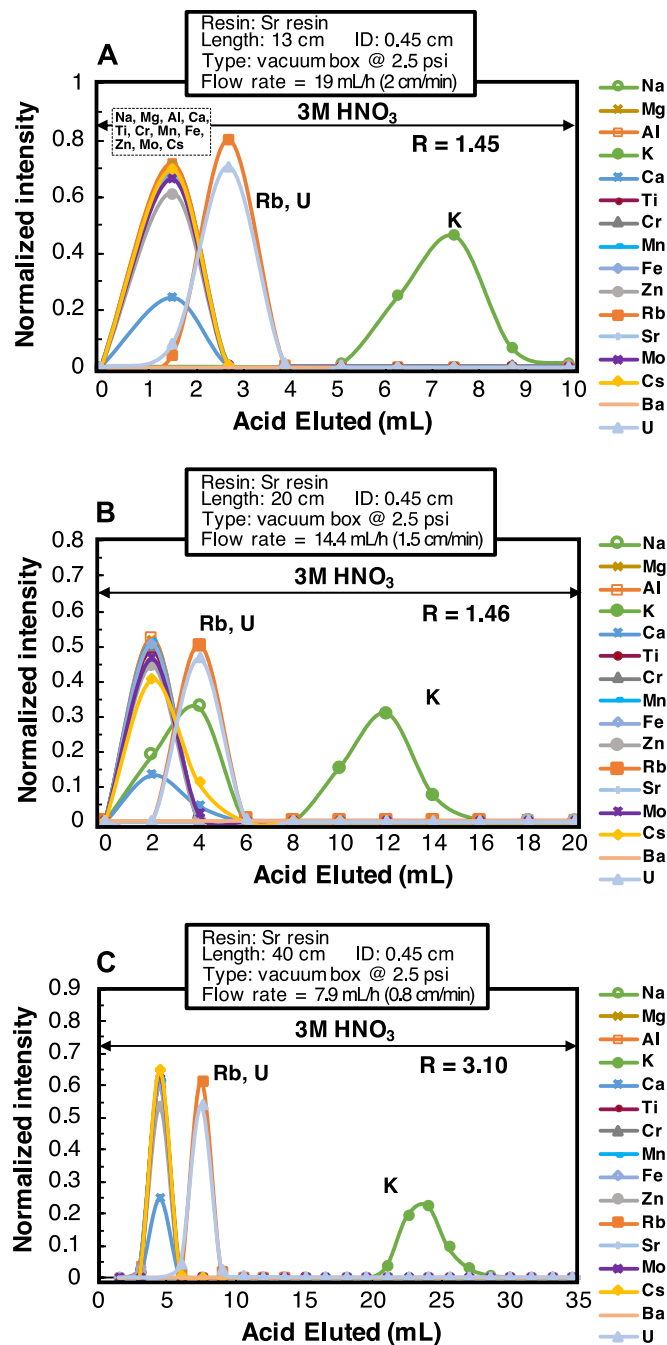


Fig. 7. Elution curves of Sr resin as a function of column length. Resolution  $R$  was calculated based on the separation between Rb and K peaks. All the tests were set at a pressure drop of 2.5 psi ( $\sim 0.17$  bar). The flow rate decreases with increasing column length, while the resolution

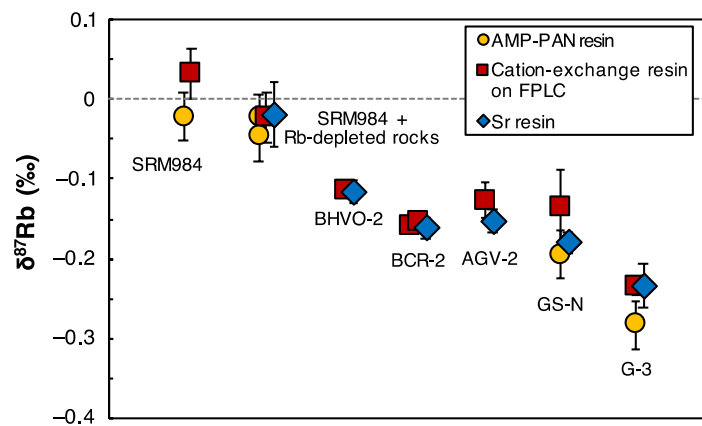


Fig. 8. Rubidium isotopic compositions of synthetic samples and geostandards, obtained using AMP-PAN method, cation-exchange resins + FPLC method, and Sr resin method (Table 1). The three methods yield consistent results. The AMP-PAN method was only applied to Rb-enriched samples such as the synthetic ones and granites due to its high Rb blank of ~80 ng. The cation-exchange resin + FPLC method and the Sr resin method have lower blanks of ~6